Ion microprobe analysis—a review of geological applications

S. J. B. REED

Department of Earth Sciences, University of Cambridge, Cambridge CB2 3EQ

Abstract

In ion microprobe analysis the specimen is bombarded with a focussed ion beam a few μm in diameter and the secondary ions produced are accelerated into the entrance slit of a mass spectrometer. An outline of the salient features of the instrument is given here, together with an account of the methods used for quantitative elemental and isotopic analysis.

The major part of this paper consists of a comprehensive account of the geological applications of ion microprobe analysis. These include elemental analysis, especially for trace elements (down to sub-ppm levels in many cases) and light elements (H–F) which are beyond the scope of the electron microprobe. The other main area of geological interest is isotopic analysis, where the ion microprobe has the advantage over conventional mass spectrometry of being capable of in situ analysis of selected points on polished sections, obviating the need for laborious specimen preparation, and enabling spatially-resolved data to be obtained, with a resolution of a few μm. The ion microprobe has been especially successful in U–Pb zircon dating and the study of isotope anomalies in meteorites. Other significant applications include diffusion and stable isotope studies.

KEYWORDS: ion microprobe, isotopic analysis, U–Pb zircon dating, meteorites.

Introduction

IN ion microprobe analysis ions focussed to form a beam (the 'primary beam') a few μm in diameter are used to bombard a solid specimen for the purpose of obtaining a localized analysis. Bombardment by primary ions removes atoms from the surface of the specimen by 'sputtering'. Some of the sputtered atoms are ionized and can be accelerated into the entrance slit of a mass spectrometer. This method of analysis is a form of 'secondary ion mass spectrometry' (SIMS), which also includes the use of relatively large-diameter primary beams for surface analysis etc. Ion microprobe analysis has several advantages over 'conventional' mass spectrometry methods, such as high spatial resolution (a few μm) and the capability for in situ spot analysis of polished sections, thereby avoiding the difficulties inherent in mineral separation.

There are many potential applications of ion microprobe analysis in geology, some of which have already been explored quite extensively, while others await further instrumental developments. The attractions of rapid in situ isotopic analysis, as compared to conventional methods involving laborious mineral separation and chemical processing, are obvious. The accuracy obtainable does not yet match that of conventional (thermal ionization) mass spectrometry, but the usefulness of the technique has already been demonstrated in various fields.

For elemental analysis the ion microprobe is from one to four orders of magnitude more sensitive than the electron microprobe, depending on the element and the matrix. Further, 'light' elements of geochemical interest (e.g. B, Be, Li and even H) are easily detectable. Elemental ion microprobe analysis entails measuring the intensity of an isotope of the element of interest and converting this into a concentration. In the absence of adequate theoretical models, 'quantification' is mainly empirical, involving comparison between elemental intensity ratios in the 'unknown' and a standard of similar composition. The use of peak intensity ratios eliminates the complex factors which affect absolute intensity. Usually the denominator is the peak intensity of a major element with known concentration (e.g. Si in silicates). Though the spatial resolution of the ion microprobe in the lateral sense is worse than for the electron microprobe (typically around

10 μm compared to 1 μm), it is much better with respect to depth, because sputtered ions originate only from the first 2 or 3 atomic layers—indeed, SIMS is widely used as a surface analysis technique. The evolution of the mass spectrum as a function of time reveals changes in composition with depth. This 'depth profiling' mode has applications in diffusion studies and the analysis of fine lamellar structures.

Instrumentation

The ion microprobe consists of a source of bombarding (primary) ions, with lenses for focussing them onto the surface of the sample. Suitable means for manipulating and viewing the sample are required so that spots for analysis can be selected. Viewing is by means of an optical microscope or an ion image. An extraction electrode in front of the sample draws the secondary ions away from the bombarded point and accelerates them towards the mass spectrometer, a system of lenses ('transfer optics') being used to focus them on the entrance slit. A schematic diagram of a typical ion microprobe is shown in Fig. 1 and the various parts are described below.

Ion source. The usual source of primary ions is a 'duoplasmatron', in which ions (e.g. Ar^+ or O^-) are produced in an arc contained by the combined influence of electrostatic and magnetic fields. These are extracted through a small aperture and accelerated by a high voltage (e.g. 10–30 kV). The yield of secondary ions can be strongly influenced by the properties of the bombarding species: thus, oxygen enhances the production of positive secondary ions because of its affinity for electrons. This applies regardless of whether O_2^- or O^- ions are used, but the latter have the advantage of minimizing charge accumulation on insulating specimens, owing to the balancing of incoming negative ionic charge by the emission of secondary electrons. Ar^+ may be used when O would cause undesirable interferences in the secondary spectrum. Sometimes it is beneficial to bombard with a strongly electropositive species (e.g. Cs^+), because this gives greater negative secondary ion intensity for electronegative elements such as S and O. Insulating specimens bombarded by positive primary ions tend to charge up, causing unstable secondary ion emission, but this can be prevented by additional bombardment with electrons from an auxiliary electron 'flood gun'.

Primary column. The primary ions are focussed onto the surface of the specimen by means of electrostatic lenses, giving a beam diameter of a few μm. With a typical beam current of several nA the rate of erosion of the sample surface is a few μm per hour. Unwanted species (e.g. OH^-)
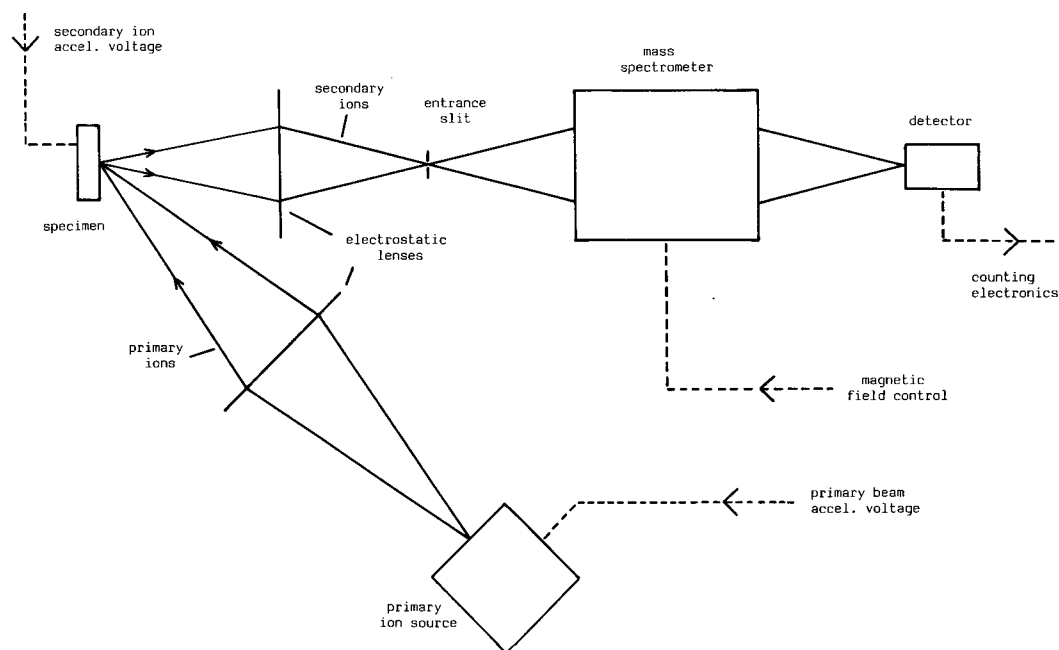

FIG. 1. Simplified schematic diagram of ion microprobe.

from the ion source can be troublesome, but primary beam mass filtering ensures that only one selected mass (e.g. ^{16}O) reaches the sample; a magnetic sector in the primary column is provided in some instruments for this purpose. It is desirable for the secondary ions to be extracted normally to the specimen surface, in order to obtain an optimum focus on the mass spectrometer entrance slit. The primary beam must, therefore, be incident at an inclined angle, as shown in Fig. 1; this is a slight inconvenience but does not cause serious difficulties.

Specimen chamber. Typically the specimens are polished sections, as used in the electron microprobe. These are coated in order to provide electrical conduction, often with carbon, though other materials (e.g. gold) may be used. A specimen holder with translational movements is required. Usually an optical viewing microscope is incorporated, though this presents some difficulties owing to the occupation of the available space by ion lenses etc.

The lowest possible pressure in the specimen chamber is desirable in order to minimize background peaks in the mass spectrum derived from water vapour or hydrocarbons. A liquid nitrogen cold trap close to the specimen helps to minimize the effect of water vapour.

Secondary ion extraction. The specimen is held at a high potential (e.g. 5 kV) relative to the grounded extraction electrode in order to accelerate the secondary ions towards the mass spectrometer. Two or more electrostatic lenses (comprising the 'transfer optics') focus the secondary ions onto the mass spectrometer slit. The size of the secondary-ion focus compared to the slit width, together with the angular divergence of the beam relative to the acceptance angle of the mass spectrometer, determine the efficiency of secondary ion collection, secondary ions with a large lateral velocity component being lost owing to their failure to pass through the slit. Discrimination between different secondary ion species can thus occur as a result of differences in their energy distributions.

The mass spectrometer. Many SIMS instruments used in other fields employ quadrupole mass spectrometers, but their mass resolution is inadequate for most geological applications, hence the magnetic sector type is preferred in this field. Maximum transmission at high mass resolution is obtained by using 'double focussing', in which an electrostatic sector combined with the magnetic sector focusses ions with different initial directions and energies.

The detector, usually an electron multiplier, is normally used in the ion counting mode, whereby each incident ion produces a discrete pulse. Detec-

tion sensitivity is a function of the fraction of sputtered atoms that are ionized and the transmission of the mass spectrometer. Typically not more than a few percent of the atoms removed from the sample reach the detector as ions.

For qualitative analysis it may be sufficient merely to sweep the magnetic field of the mass spectrometer while recording the detector output in analogue form. However, for quantitative analysis, computer control of the magnetic field and digital recording of the spectrum are necessary. At high mass resolution a field setting accuracy of a few parts per million is required.

High mass resolution enables small differences in mass between peaks of interest and interferences to be exploited. The mass resolution (defined as mass divided by peak width) needed for this purpose varies quite widely, but mostly lies in the range 2000–7000. Such resolution requires the mass spectrometer slits to be narrow, hence there is an unavoidable reduction in sensitivity. In this regard a large mass spectrometer is advantageous since the slit width is greater for a given resolution.

An alternative approach to the problem of molecular interferences is energy filtering, which exploits the fact that atomic ions exhibit a 'tail' extending to relatively high energies, whereas very few molecular ions possess energies greater than a few eV, since they tend to dissociate if ejected with higher energy (Fig. 2). It is thus possible to discriminate against molecular species by accepting only high-energy secondary ions, though a substantial intensity loss is entailed, since the
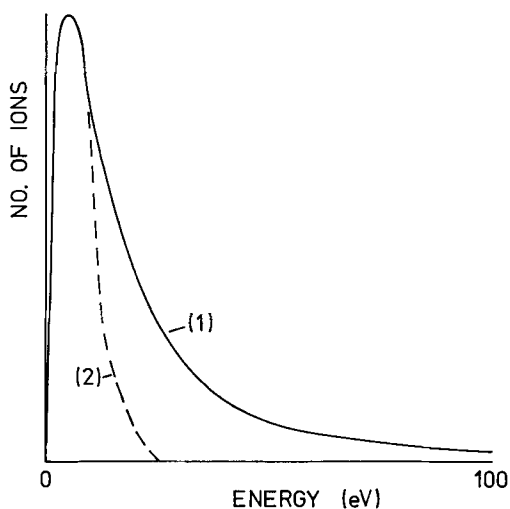

FIG. 2. Energy distributions of (1) atomic and (2) molecular secondary ions.

majority even of atomic ions have energies below the discrimination threshold, as set to a typical level (e.g. 50 eV). Energy filtering is achieved by means of a slit located after the electrostatic sector of the mass spectrometer; the mean transmitted energy is usually controlled by varying the accelerating potential on the sample.

Imaging. In the direct-imaging secondary-ion microscope (Castaing and Slodzian, 1962) a relatively large area (e.g. 300 μm diameter) is bombarded and an image of this area is formed on a fluorescent screen by the secondary ions after they have passed through the mass spectrometer, showing the spatial distribution of the selected isotope or element. Images can also be produced by scanning a focussed ion beam across the sample. Direct imaging is more efficient than scanning because the whole image is formed simultaneously rather than on a point-by-point basis. The ion microscope can be used as a microprobe either by focussing the primary beam to the required diameter or selecting a small part of the image using an aperture.

List of instruments. The following ion microprobe instruments have been used in geology.

(i) ARL IMMA (Liebl, 1967). This instrument, manufactured in the USA, was used quite extensively in early explorations of geological applications of the technique. It was handicapped by the lack of high mass resolution capability.

(ii) Hitachi IMA-2 (Tamura *et al.*, 1970). Somewhat similar in performance to the ARL IMMA, this instrument has been used in Japan for several geological applications.

(iii) AEI IM-20 (Banner and Stimpson, 1974). Manufactured in the UK, this instrument had the advantage of high mass resolution (up to about 8000). In spite of its relatively low sensitivity, it has been employed quite effectively over a wide range of applications.

(iv) Cameca IMS-300 (Castaing and Slodzian, 1962). This was the first commercial version of the direct imaging ion microscope, as described in the previous section. A number of geological applications of secondary ion imaging using this instrument were published and it was also used to a limited extent for quantitative microprobe analysis.

(v) Cameca IMS-3f (Lepareur, 1980). This radically redesigned successor to the IMS-300 has been superseded by the IMS-4f (Migeon *et al.*, 1986), which incorporates a number of relatively minor improvements. The mass resolution capability of around 10000 is similar to that of the AEI IM-20, but the sensitivity is higher. For several years this instrument has been the only high performance ion microprobe commercially available and it has been installed in a number of geological laboratories.

(vi) ANU SHRIMP (Compston *et al.*, 1982). This instrument, designed and built at the Australian National University, Canberra, incorporates a very large mass spectrometer giving exceptionally high sensitivity at high mass resolution, and has been applied mostly to the U-Pb dating of zircons.

Quantitative analysis

The usual objective of ion microprobe analysis is to determine either the concentrations of the elements present, or relative isotope abundances, in the small volume of sputtered material. In either case it is essential that the measured peaks should be free from interferences, which, if present, require the use of either high mass resolution or energy filtering. In some cases measurements made at low mass resolution can be corrected for interferences by 'spectrum stripping', whereby the contribution of an interfering molecular species is estimated from the observed intensity of a neighbouring peak of the same species but with a different combination of isotopes. This approach has the advantage of avoiding the intensity loss inherent in the methods mentioned above, but is only applicable where the interferences are not too large and are fully identifiable.

In measuring peak intensities a sufficient number of ion counts must be recorded to give adequate statistical precision; also the dead-time of the counting system must be taken into account. In order to convert peak intensities into elemental concentrations, one needs to know the 'relative sensitivity factors' for the elements concerned. In isotopic analysis, mass fractionation may occur in the production, collection and detection of the secondary ions, and must be allowed for.

Elemental analysis. An elemental analysis is normally based on the measured intensity of a single isotopic peak of the element concerned. For elements with several isotopes, the most intense is selected as a rule, though sometimes an alternative choice may be advantageous with regard to minimizing interferences. Absolute intensities are not very reproducible; hence it is usual to measure the ratio of the peak intensity of the element of interest to that of another element, the concentration of which is known (e.g. Si in silicates). Relative sensitivity factors are dependent not only upon the properties of the elements concerned (mainly the ionization potential) but also on the matrix.

The development of theoretical models for calculating secondary-ion yields has been hampered by the complexity of the processes involved. In the 'local thermal equilibrium' (LTE) model of

Andersen and Hinthorne (1973a), it is assumed that the secondary-ion source region is, or behaves like, a plasma, i.e. a high-temperature assemblage of free atoms, ions and electrons, allowing the application of plasma equations to predict ion yields. However, the theoretical basis of the LTE model is dubious, and it is not universally successful in practice. It has thus fallen out of favour and purely empirical methods are generally used.

Matrix effects can be avoided by using a standard close in composition to the 'unknown', though it is impossible to know a priori how close the composition needs to be. It is often difficult to obtain trace element standards, but the problem is eased somewhat if it can be assumed that ion yield is independent of concentration, which appears to be true for concentrations up to the percent level. Thus it is valid to use a standard containing the element of interest at a concentration high enough to be determined with the electron microprobe, even though the concentration in the analysed material may be much lower.

Ray and Hart (1982) obtained linear working curves for a number of elements with concentrations ranging from 25 to 500 ppm in diopside–albite–anorthite glasses. The data points plotted on the same set of straight lines, i.e. no matrix effects were found. However, measurements on crystalline samples of similar composition showed differences in relative ion yield averaging 30%, indicating the need for caution in using glass standards.

It cannot be assumed that matrix effects are always small; thus, Shimizu et al. (1978) observed that the sensitivity for Al relative to Si differs appreciably in different silicates. Also quite large variations in the relative ion yields of major elements in olivines and low-Ca pyroxenes have been observed (Shimizu et al., 1978; Steele et al., 1981), and the ion yield of trace Ni in these phases depends quite strongly on the Fe/Mg ratio (Reed et al., 1979; Steele et al., 1981).

In an attempt to systematize matrix effects in silicates, Havette and Slodzian (1980, 1982) proposed that the ion yield of element 'x' relative to Si, defined as:

$$^xR_{Si} = (I_x/C_x)/(I_{Si}/C_{Si}),$$

where I_x and I_{Si} are the peak intensities for 'x' and Si, and C_x and C_{Si} are their concentrations, may be expressed as a linear function of the concentrations of the matrix elements, thus:

$$^xR_{Si} = \Sigma C_i \cdot {}^xK_i.$$

The coefficients ^xK_i represent the influence that element i has on the relative ion yield of element x and are determined empirically from measure-

ments on standards. For 25 Al-containing silicates it was found that $^{Al}R_{Si}$ varied from 4 to 13.

Slodzian (1982) showed that the linear behaviour of ion yields as a function of concentration is consistent with a bond-breaking model for the ionization process, which also explains certain aspects of isotopic fractionation (see below). The model, however, has not yet been developed to the stage where matrix effects for complex samples can be predicted.

It should be noted that relative sensitivity factors are dependent on instrumental characteristics (in particular the energy 'window' for secondary ions). Energy discrimination, as used for suppressing molecular interferences, significantly affects relative sensitivities (in general, ion yield differences are reduced).

An interesting approach to the problem of standards is ion implantation (Leta and Morrison, 1980). A known 'dose' of an isotope of the element of interest is introduced into the sample by bombardment with high-energy ions prior to analysis. The integrated signal for this isotope obtained in the depth profiling mode while sputtering through the implanted region (usually within the first μm in depth) enables the sensitivity for that particular element/matrix combination to be determined. This method has been applied to surface layers of lunar silicates (Zinner and Walker, 1975; Zinner et al., 1976), Li in various phases (Wilson and Long, 1982), and to the determination of Ag and Au in sulphide ores (Chryssoulis et al., 1986, 1987). A variation on this technique is to carry out the implantation in the ion microprobe itself, using special ion sources to provide the required species (Streit et al., 1986).

The advantage of the ion microprobe over other analytical techniques lies chiefly in its spatial resolution, but it can also be used for bulk analysis. Nesbitt et al. (1986) described a whole-rock analysis procedure in which rock powder samples were mixed with Pb_2SiO_4 and fused to form glasses. Working curves derived from 6 international rock standards were used for quantification, the accuracy being about $\pm 5\%$ for major and $\pm 10\%$ for trace elements.

Isotopic analysis. In measuring isotope abundances, many of the factors requiring consideration (e.g. molecular interferences) are the same as in elemental analysis. Instrumental discrimination and matrix effects are much smaller in the case of measurements of different isotopes of the same element, but much higher accuracy is required (e.g. $\pm 0.1\%$), hence relatively small effects are important.

In general, measured isotope ratios differ from true ratios on account of mass discrimination both

in the ionization process and in the instrument itself. Slodzian *et al.* (1980) measured Mg, Si and Ca isotope ratios in natural materials and found discrimination of the order of 1% per mass unit, with the lighter isotopes enhanced. Mass fractionation was found to be dependent on the band of secondary-ion energies selected, low energies showing the greatest effects. Significant matrix effects were observed; for example, the mass fractionation of Ca was found to be much smaller in calcite than in feldspar. These results were shown to agree qualitatively with the bond-breaking ionization model mentioned above.

Similar conclusions have been reached by others; for example, Lorin *et al.* (1982) observed mass fractionations of 1.5% to 3.7% per mass unit for Mg in different minerals, 3.6–6.4% for Si, and 0.25–2.0% for Ca. Shimizu and Hart (1982) conducted measurements on 13 pure metallic samples ranging from B to Pb, confirming the existence of a significant dependence on secondary-ion energy, with mass fractionation ranging from 0.6% per mass unit for Pb to 6.5% for B, the effect being largest for light elements because the relative mass difference of the isotopes is greatest.

The energy dependence of mass fractionation can be put to good use, by selecting high-energy ions in the mass spectrometer in order to reduce matrix effects. However, a degree of discrimination also occurs in the transfer of secondary ions from the sample to the mass spectrometer, and measured isotope ratios may be affected by the 'retuning' of various instrumental parameters required on moving from one point to another. This effect can be minimized by ensuring that specimens and standards are flat and co-planar.

Obviously the precision of isotope ratio measurements is determined by counting statistics, but even with abundant ion counts the accuracy obtainable with the ion microprobe appears to be limited at present to about $\pm 0.1\%$. Though adequate for many purposes, this accuracy is inferior to 'conventional' (e.g. thermal ionization) mass spectrometry. The usefulness of the ion microprobe is thus dependent on its particular advantages, namely spatial resolution, the small amount of material consumed, minimal sample preparation and high output rate.

Applications

Light elements. 'Light' elements (below 10 in atomic number), which are difficult, if not impossible, to determine quantitatively with the electron microprobe, are easily detectable with the ion microprobe. Also, they are to a large extent free from interferences and where these do occur they are usually easily resolved; for example, a mass

resolution of 500 is enough to separate ^{9}Be from ^{27}Al^{3+} and ^{10}B from ^{30}Si^{3+}. Secondary ion yields are reasonably high for light elements of geochemical interest such as Li, Be, B and F, enabling sub-ppm detection limits to be attained. The determination of H is a useful application of the ion microprobe, but special precautions are needed to minimize the background level of H originating from residual water vapour in the specimen chamber.

Early applications included the determination of Li and B in Apollo 11 lunar samples by Andersen *et al.* (1970), Li in lunar plagioclase by Meyer *et al.* (1974) and Steele *et al.* (1980a), and Li, Be, B and F in aluminous lunar glasses by Meyer (1978). Phinney *et al.* (1979) determined Li, Be and B in Allende meteorite material, while Steele *et al.* (1980b) included these elements and F in a comprehensive study of trace elements in terrestrial plagioclase. Hinthorne and Andersen (1975) obtained working curves for H and F in silicates from measurements on a number of previously analysed mineral samples.

The ion microprobe is useful for determining light elements 'missing' in electron microprobe analyses, as in the study of B in the humite-group orthosilicate, chondrodite, by Hinthorne and Ribbe (1974). The concentration of B was found to be correlated with Si deficiency in the electron microprobe data. The substitution of B for Si in sillimanite was studied by Grew and Hinthorne (1983); concentrations of up to 0.43% B_2O_3 were found in samples from high temperature B-rich environments.

Other light element studies include measurements of Li in olivine and orthopyroxene in harzburgites, the estimated detection limit being 10 ppb (Hervig *et al.*, 1980a). The distribution of various trace elements, including Li, in feldspars was investigated by Mason (1982), while Mason *et al.* (1982) determined Li and B in anorthoclase megacrysts. Steele *et al.* (1981) determined Li in olivines and low-Ca pyroxenes. Jones and Smith (1984) studied H, Li, B and F in micas and some other phases. A study of Li in different minerals in granites from Cornwall was reported by Wilson and Long (1983). Concentrations ranged from percent levels in some micas down to less than 1 ppm in topaz and some feldspars. Ion implantation was used to determine matrix effects.

In recent work by Dutrow *et al.* (1986) Li and F were determined in staurolites, and the significant role of Li in this phase was confirmed. Holdaway *et al.* (1986) used the ion microprobe to determine H in staurolites previously analysed by mineral separation and H extraction. The H concentrations were in the region of 2% and a

peak to background ratio of more than 30:1 was obtained (background being determined on meteoritic olivine).

Grew et al. (1986) determined Li, Be, B and F in margarite and paragonite (Ca and Na-rich micas respectively) from Antarctica. The standards used were spodumene (Li), surinamite (Be), grandidierite (B), and biotite (F). Matrix effects were assumed to be negligible, and the measurements were made at low mass resolution.

Ion microprobe determination of Li and B in topaz from different geological settings by Hervig et al. (1987) showed Li and B to vary over a wide range. High Li (and to a lesser degree B) was found to be correlated with an igneous origin (see Fig. 3).
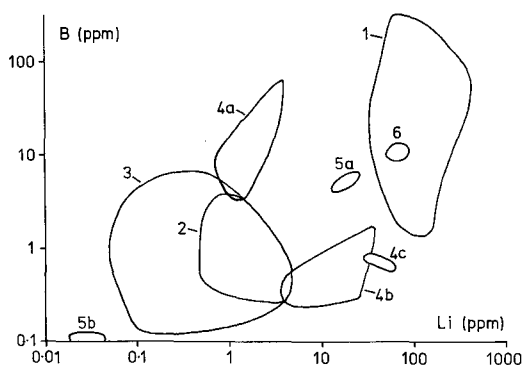

FIG. 3. Ion microprobe data for Li and B in topaz from different environments; key: 1—rhyolites, 2—pegmatites, 3—hydrothermal greisens, 4a, b, c—various metamorphics, 5a, b—topazites, 6—ongonite (after Hervig et al., 1987).

Trace elements. For geochemical trace element analysis it is usual to employ techniques such as neutron activation or atomic absorption, which have good sensitivity but lack spatial resolution and are dependent on mineral separation procedures which are sometimes less than perfect. The ion microprobe enables trace elements to be determined in a very similar fashion to the electron microprobe, but with detection limits lower by from 1 to 3 orders of magnitude.

This section is concerned with the application of the ion microprobe to 'ordinary' trace elements, excluding the 'light' elements covered in the preceding section and rare earths, which are treated separately in the following section. Some of the earliest applications involved lunar sample analysis, where the low sample consumption is particularly advantageous. For example, Andersen et al.

(1970) analysed major phases in Apollo 11 rocks and investigated zoning patterns. Plagioclase in lunar samples was analysed by Meyer et al. (1974); spectrum stripping was used to correct Rb and Sr data obtained at low mass resolution. Later work on lunar samples by Steele et al. (1980a) exploited the high mass resolution capability of the AEI instrument to investigate interferences, which were found to be small for Mg, K, Ti, Sr, and Ba at the concentrations present.

In the related field of meteoritics, Reed et al. (1979) investigated the partitioning of Ni between olivine and metal in pallasites, the concentration in olivine being low compared to typical terrestrial olivines, at around 25 ppm. A mass resolution of 2000 was used to separate the ^{60}Ni peak from $^{28}Si^{16}O_2$. Measurements on terrestrial olivines of known composition revealed a quite strong dependence of Ni^+/Fe^+ ion yield ratio on Fe/Mg ratio. In iron meteorites Ga is of interest in view of its systematic variation between different classes. Ion microprobe measurements showed it to be highly concentrated in the taenite phase (Reed and Enright, 1981). The ^{69}Ga peak is affected by a small molecular interference, necessitating the use of high resolution for concentrations below a few ppm. Further studies of iron meteorites have been reported by Okano and Nishimura (1982), who recorded profiles of Ni, Co, Ga, and Cu across kamacite and taenite grains.

The partitioning of Ga between metal and silicate (representing the core and mantle of planetary bodies) was investigated experimentally by Drake et al. (1984). Metal and silicate standards containing varying amounts of Ga were used and a large matrix effect was observed, the Ga^+ ion yield relative to Fe^+ being about 10 times higher in metal than in silicate. Another experimental study was reported by Steele and Lindstrom (1981), who measured Ni partitioning between diopside and silicate melt. A linear relationship between $^{58}Ni^+$ intensity and Ni concentration in previously analysed samples was found for concentrations up to 1%, but a difference in relative Ni^+ yield in different silicates was observed.

Trace elements in natural terrestrial samples have formed the subject of a considerable number of published papers. Several studies of feldspars have been reported; for example, plagioclase from different magmatic environments was analysed by Shimizu (1978) for Mg, K, Fe and Sr, using energy filtering to suppress interferences, the estimated accuracy for these elements being 5–10%. Mason et al. (1982) determined the concentrations of several minor and trace elements in anorthoclase megacrysts from 5 locations. Inspection of peaks at high mass resolution showed ^{24}Mg, ^{49}Ti, ^{133}Cs,

and ^{138}Ba to be practically free of interferences, allowing measurements to be made at low mass resolution, whereas ^{56}Fe, ^{85}Rb, and ^{88}Sr had to be recorded at high mass resolution. Further work by Mason (1982) involved the determination of trace element partitioning between K-feldspar and albite in perthites from pegmatites; within-grain zoning was also studied.

Cerny et al. (1984) reported a detailed study of feldspar crystallization in a pegmatite, the distributions of a number of trace elements being determined and their fractionation trends in the crystallization sequence investigated. Mason et al. (1985) carried out a study of minor and trace element distributions in alkali feldspars from the Klokken (S. Greenland) layered syenite series. Elements determined included Mg, P, Ti, Rb, Sr and Ba.

Transition element distributions in garnet lherzolite nodules in kimberlites were determined by Shimizu and Allègre (1978). Data for Sc, Ti, V, Cr, Mn, Co, Sr, and Zn in clinopyroxene and garnet were used to assess the possibilities of geothermometry and geobarometry, and it was concluded that V and Mn in particular were potentially useful. The trace element data also suggested classification of these nodules into three groups, one possibly representing near-pristine mantle.

Analyses of Cr–Al-spinel harzburgite xenoliths from kimberlites, including ion microprobe data for trace elements, revealed two chemical groups (Hervig et al., 1980a). In 'fertile' harzburgites the orthopyroxenes showed higher levels of Li, Cr, Ca and Al compared to those classified as 'barren', both having compositions distinct from garnet and spinel lherzolites. Hervig et al. (1980b) also used the ion microprobe to determine a number of trace elements in silicate inclusions in diamonds.

Shimizu (1981) investigated the spatial distribution of a number of trace elements in a sector-zoned augite phenocryst to see if kinetic effects on partitioning were detectable. The observation that the slower-growing sector was enriched in trace elements was used to choose between crystallization models. Recently a further study of zoning in augite phenocrysts has been completed (Shimizu and le Roex, 1986).

Analyses of Cu in biotites, amphiboles and magnetites in intrusive rocks of the Koloula igneous complex (Solomon Islands) have been reported by Hendry et al. (1981). The ^{63}Cu peak was measured at a mass resolution of 2000 in order to avoid interferences. Data from silicate glass standards showed a strong dependence of the Cu^+/Fe^+ ion yield ratio on Fe concentration. Concentrations of Cu down to about 1 ppm were measured. The results suggested that the associated porphyry copper deposits originated by extraction of Cu from the silicates by boiling hydrothermal fluids. A later study of a number of N. American porphyry copper deposits, however, indicated a different origin (Hendry et al., 1985).

The distribution of trace elements in ores is of potential economic interest. McIntyre et al. (1984) investigated the viability of the ion microprobe technique for determining Ag and In in sulphides. Calibration plots were obtained from synthetic standards; detection limits were 5 ppm Ag and 0.5 ppm In (with a counting time of less than one minute). Energy filtering was used to suppress interferences. Several natural galena and sphalerite grains from Baffin Island (Canada) were analysed.

Chryssoulis et al. (1985, 1986) applied the ion probe to the determination of Ag at low concentration levels in sulphide ores, using ^{109}Ag for analysis and at the same time measuring the intensity of ^{107}Ag introduced by ion implantation for the purpose of calibration. An accuracy of around $\pm 15\%$ was obtained for Ag concentrations of a few ppm. A similar approach was used by Chryssoulis et al. (1987) in order to determine Au in sulphides.

Veizer et al. (1987) investigated the application of the ion microprobe (AEI IM-20) to trace elements (Na, Mg, Mn, Fe, Sr) in calcite and dolomite. Ion yields for many elements are low in carbonates; for example, in this study the yield of Fe^+ was found to be only 4% of that of Ca^+. Mason (1987) investigated the relationship between trace elements and cathodoluminescence zonation patterns in limestone cements.

Okano and Uyeda (1988) reported the application of the ion microprobe to the determination of U in fossils, the spatial resolution being better than that obtained by the usual technique of fission track counting. In fossil horse teeth the U content was shown to be higher in dentine than in enamel.

As well as measuring natural trace element distributions, the ion microprobe is applicable to experimental partitioning studies, the low detection limits enabling possible departure from Henry's law at low concentrations to be investigated. In a study of clinopyroxene–liquid partitioning of Sc, Ti, Sr and Sm, Ray et al. (1983) found that Henry's law was obeyed over concentration ranges typical of natural systems.

Rare earths. The rare earth elements (*REE*) are of considerable geochemical interest. The electron microprobe, with detection limits in the region of a few hundred ppm for these elements, is of limited usefulness. By comparison, the ion microprobe offers much lower detection limits, while avoiding the necessity for the laborious separation pro-

cedures required by techniques such as neutron activation analysis.

Two kinds of molecular interference are important in *REE* determination: firstly the oxides of light *REE* (*LREE*), which are superimposed on the heavy *REE* (*HREE*) peaks, and secondly molecules composed of combinations of matrix atoms (e.g. Ca, P, O in the case of apatite). Separation of *HREE* peaks from *LREE* oxides requires fairly high mass resolution (around 8000) and energy discrimination is not very effective in suppressing *REE* oxides. Matrix molecules, on the other hand, are easier to eliminate by either method.

As in the case of other ion microprobe applications, lunar samples were amongst the first objects of study. Andersen and Hinthorne (1972) investigated the distribution of *REE* in various lunar accessory phases in which the concentrations were high enough for matrix interferences to be unimportant. Only the light *REE* (La–Eu) were included, in order to avoid the problem of *LREE* oxide interferences. Lovering (1975) applied a similar approach to *REE* in terrestrial zirconolites.

Usually the most significant aspect of *REE* is the shape of the plot obtained by normalizing the concentrations relative to chondritic meteorites, the absolute concentrations being less important. To determine relative *REE* concentrations with the ion microprobe, knowledge of their relative ion yields is required. In early work the ion yields of *REE* were assumed to be all the same; for example, Shimizu *et al.* (1978) analysed hornblendes and Gaudette *et al.* (1981) analysed zircons using this assumption.

Shimizu and le Roex (1986) obtained *REE* distribution plots for augite phenocrysts from Gough Island alkaline basalts. Energy filtering was used and *REE* isotope ratios were measured to test for interferences. The six most readily detectable and interference-free *REE* were included and for these a constant ion yield was assumed. A previously analysed diopside with *REE* concentrations down to 0.44 ppm gave reasonably satisfactory results.

Measurements on artificial glass standards containing known *REE* concentrations demonstrate the existence of quite large differences in ion yield amongst the *REE* (Reed, 1981, 1983). These appear to be related more to oxygen affinity than ionization potential, but it does not seem that any simple model fits the experimental data, hence it is necessary to use empirical quantification procedures.

REE oxide interferences can be avoided by using the oxide peaks of the *HREE* for analytical purposes, together with the atomic peaks of the *LREE* (Reed, 1981). This approach has been applied to the determination of complete *REE* distributions in allanites (Reed, 1985). The ion yields were obtained from an allanite standard analysed by neutron activation. Measurements made at low mass resolution were corrected for interferences from matrix molecules using factors derived from peak profiles recorded separately at high resolution. The application of this approach to other *REE*-bearing accessory phases has been described by Reed (1986). Results for perovskite have been reported recently by Mitchell and Reed (1988).

Measurements of *REE* concentrations in the phosphate phases apatite and merrillite in chondritic meteorites (Reed *et al.*, 1983) disproved earlier results obtained by mineral separation and neutron activation analysis. The marked partitioning of *REE* in favour of merrillite revealed by the ion microprobe is significant in connection with the use of *REE* to infer Pu partitioning in the context of Pu–Xe dating. Owing to the limited sensitivity of the AEI instrument used it was not feasible to inspect the peaks of *HREE* in apatite at high resolution. In a further study, 15 chondrites were analysed, the measurements in this case being restricted to La–Nd in merrillite and Ce in apatite (Reed and Smith, 1985).

More complete analyses of chondritic apatite, as well as merrillite, were obtained by Crozaz and Zinner (1985), using a Cameca IMS-3f instrument, with energy filtering. A spectrum stripping procedure was used to extract the required peak intensities from the complete overlapping spectrum of the *REE* and their oxides. The detection limits obtained were well below 1 ppm. The technique has been described in greater detail and applied to meteoritic hibonite by Zinner and Crozaz (1986). Fahey *et al.* (1987*c*) analysed perovskite and melilite in Ca-Al-rich inclusions in the Efremovka carbonaceous chondrite for *REE* using this method.

Relatively little work on *REE* in rock-forming silicates has been reported so far, though the available sensitivity is adequate at least in some cases. Zinner and Crozaz (1986) analysed meteoritic pyroxene, obtaining good agreement with INAA data. The concentrations were in the range 0.3–20 ppm (20–30 times chondritic). *REE* patterns in garnet inclusions in peridotite-suite diamonds were determined by Shimizu and Richardson (1987) using energy filtering for interference suppression. The concentrations were mostly in the range 1–10 times chondritic.

MacRae and Metson (1985) used an extreme form of energy filtering obtained by electrical isolation of the specimen, which reaches a negative

potential of several hundred volts (under bombardment by negative primary ions). Only a small fraction of the positive secondary ions have enough energy to escape from the specimen. The high threshold energy ensures very efficient suppression of molecular interferences, including *REE* oxides. The disadvantage of this mode of operation is that there is a significant loss of spatial resolution as well as intensity. Pyroxenes and plagioclases with *REE* concentrations in the range 10–100 times chondritic were analysed. Muir *et al.* (1987) compared results obtained for *REE* in monazite and augite by the specimen isolation method and by conventional energy filtering, while MacRae and Russell (1987) applied the former method to the determination of *REE* in komatiite pyroxenes, and MacRae (1987) applied it to whole-rock analysis using fused powder samples.

Isotopic analysis—Pb. The capability of the ion microprobe for rapid *in situ* isotopic analysis of small selected areas is obviously of great interest in geology. One of the most fruitful fields of application is Pb isotopes, the natural variation in $^{207}Pb/^{206}Pb$ ratios being relatively large. However, in the case of zircon (the most important host phase with regard to dating) the low Pb concentration and the presence of molecular interferences create considerable difficulties.

Measurements by Andersen and Hinthorne (1972, 1973*b*) of 207/206 ratios in various lunar phases including zircon, zirkelite and phosphates, gave approximate ages in the region of 4 Gyr. No 204 peak was detected and therefore no common-Pb correction to the 207/206 ratios was applied. The measurements were made at low mass resolution using an ARL instrument, and were corrected for interferences by spectrum stripping. Measurements of 207/206 ratios on artificial standards showed a reproducibility of ±0.4%, as limited by counting statistics (Andersen and Hinthorne, 1973*a*).

Further measurements on standards (Hinthorne *et al.*, 1979) showed that instrumental mass fractionation was not significant, though it was found necessary to use a cold trap to minimize hydride interferences (most importantly $^{206}Pb^1H^{-207}Pb$). In high-U phases (e.g. uraninite) molecular interferences were found to be small and plausible ages were obtained from uncorrected 207/206 ratios. For zircons a more rigorous peak stripping procedure was used than previously; the 9 peaks from 202 to 210 were measured, assuming 9 components to be present (5 molecular species and 4 Pb isotopes). Ion microprobe data for two zircon samples were in good agreement with previously determined ages of 1.0 and 2.8 Gyr.

Lovering *et al.* (1981) analysed zircons from

rocks in Australia and Antarctica on either side of the supposed rift in the Gondwanaland Precambrian shield. The results supported the rifting hypothesis, ages ranging from 1.6 to 3.5 Gyr being found on both sides, the older dates probably representing material derived from the adjacent Archaean rocks. The stripping procedure described above was used. In a few cases significant errors due to additional molecular interferences involving minor elements were observed.

Vander Wood and Clayton (1985) extended the stripping procedure to include additional molecular species, requiring 11 peaks (201–211) to be measured. Although other interferences (e.g. Y_2O_2, $REEO_2$) can occur in this mass region, it was deduced that neither these nor the presence of common Pb could account for the range of 207/206 ratios observed in Antarctic Archaean zircons. In particular it was concluded that 207/206 ratios significantly higher than the mean represented a component older than the 2.5 Gyr inferred from conventional bulk analysis. The ion microprobe was also applied to zircons from the Abitibi (Canada) greenstone belt, with ages around 2.8 Gyr.

The uncertainties inherent in spectrum stripping can be avoided by employing high mass resolution. Hinton and Long (1979), using an AEI instrument, found a resolution of 3200 to be sufficient to separate the most important interfering species. Measurements on separated zircons from a tonalite gneiss from Lac Seul, Ontario, showed a wide range of 207/206 ratios, with cores apparently older than rims, and inferred ages extending up to 3.5 Gyr, compared to a minimum age of 3.0 Gyr determined by conventional methods. The ^{204}Pb peak could only be detected by using long counting times for a few selected grains, on the basis of which it was concluded that the effect of common Pb on the 207/206 ratios was small.

For complete separation of the isotopic peaks of Pb from molecular interferences, somewhat higher mass resolution is desirable, but with nearly all current instruments the associated intensity loss is severe. In the ANU SHRIMP instrument, described in a previous section, the large mass spectrometer gives high sensitivity at its usual working mass resolution of about 7000 (see Fig. 4). This instrument has been used extensively for zircon dating.

The usefulness of Pb isotope data is enhanced if the U/Pb ratio is also measured, thereby enabling 'concordia' plots to be obtained. However, the measurement of U/Pb ratios is hindered by the large and variable discrimination factor between U and Pb (probably related to their widely differing secondary-ion energy distributions). The ANU

group have applied a method for correcting measured U^+/Pb^+ ratios proposed by Hinthorne et al. (1979), using an empirical factor which is a function of the measured UO^+/U^+ ratio. Initially the accuracy of the U/Pb ratios obtained was $\pm 5\%$, but recently this has been improved to better than $\pm 2\%$ (Williams and Claesson, 1987).
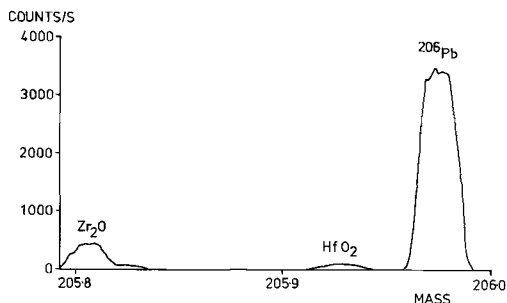

FIG. 4. The 206 peak from a zircon containing 180 ppm Pb, recorded at a mass resolution of 6500 using the 'SHRIMP' instrument.

The value of the ion microprobe for U–Pb dating of zircons has been demonstrated in a series of papers by the ANU group. Perhaps the most notable result obtained so far has been the discovery of the oldest known terrestrial zircons, with ages of 4.1–4.2 Gyr (Froude et al., 1983). The ion microprobe was used to analyse a large number of detrital grains from Mount Narryer (W. Australia) individually; only a very small proportion were found to have 'old' cores, the majority having been completely reset by later metamorphism. Even older zircons (4.28 Gyr) from another locality in W. Australia were dated subsequently by the same technique (Compston and Pidgeon, 1986). These observations help to define the time interval between the formation of the Earth and the appearance of continental crust.

In a study of zircons from the granodioritic orthogneiss of Mt. Sones, Enderby Land, Antarctica, Williams et al. (1984) were able to show the existence of excess radiogenic Pb in small regions of some grains, giving rise to 'reverse discordance', i.e. points lying above the concordia line as opposed to 'normal' discordance caused by Pb loss (Fig. 5), demonstrating the need for caution in interpreting conventional 207/206 data. In a further study of Mt. Sones zircons (Black et al., 1986), four major events were identified: original zircon emplacement at 3.93 Gyr; some recrystallisation at 2.95 Gyr due to metamorphism; extensive Pb movement at 2.48 Gyr, with some new zircon

growth; and further disturbance at about 1.0 Gyr associated with tectonic activity. This is a good example of the ability of the ion microprobe to unravel complex sequences of events.

The ANU instrument has also been applied to the dating of zircons from various other localities, as follows:

Kambalda volcanics, W. Australia (Compston et al., 1986b);
Amitsoq gneiss, Greenland (Kinny, 1986);
Isua supracrustals, Greenland (Compston et al., 1986a);
Archaean granites, W. Australia (Compston et al., 1986c);
Crustal xenoliths, Queensland, Australia (Rudnick and Williams, 1987);
Granitoids, New Hampshire (Harrison et al., 1987);
Paragneisses, Seve Nappes, Sweden (Williams and Claesson, 1987);
Late Precambrian ejecta blanket, S. Australia (Compston et al., 1987);
Tonalite gneiss, Swaziland (Compston and Kröner, 1988);
Dengfeng greenstone, China (Kröner et al., 1988a);
Barberton greenstone, S. Africa (Kröner and Compston, 1988);
Anorthosites and orthogneisses, W. Australia (Kinny et al., 1988);
Moldanubian sediments, Czechoslovakia (Kröner et al., 1988b);
Kambalda greenstones, W. Australia (Claoué-Long, et al., 1988).

As far as the measuring technique is concerned, U–Pb dating of uraninite or pitchblende with the ion microprobe is much less demanding than zircon, owing to the high Pb concentration (typically a few percent). Reed et al. (1988) have reported measurements on pitchblende from the Olympic Dam ore deposit, S. Australia, using the ion microprobe for the Pb isotopes and electron microprobe analysis of the same spots for determining U/Pb ratios.

Some ion microprobe work on Pb isotopes in galena has been reported. Shimizu et al. (1978) obtained a precision of $\pm 0.1\%$ in 207/206 ratios, and an absolute accuracy of $\pm 0.5\%$, as estimated from measurements on a previously analysed standard, using a Cameca IMS-300. A series of point analyses on a large galena crystal from Picher, Mississippi Valley, revealed oscillatory isotopic variations (Fig. 6), compared with the monotonic variation recorded previously using conventional methods. Hart et al. (1981) constructed an isotopic 'contour map' of a Mississippi Valley-type galena crystal from a large number of point
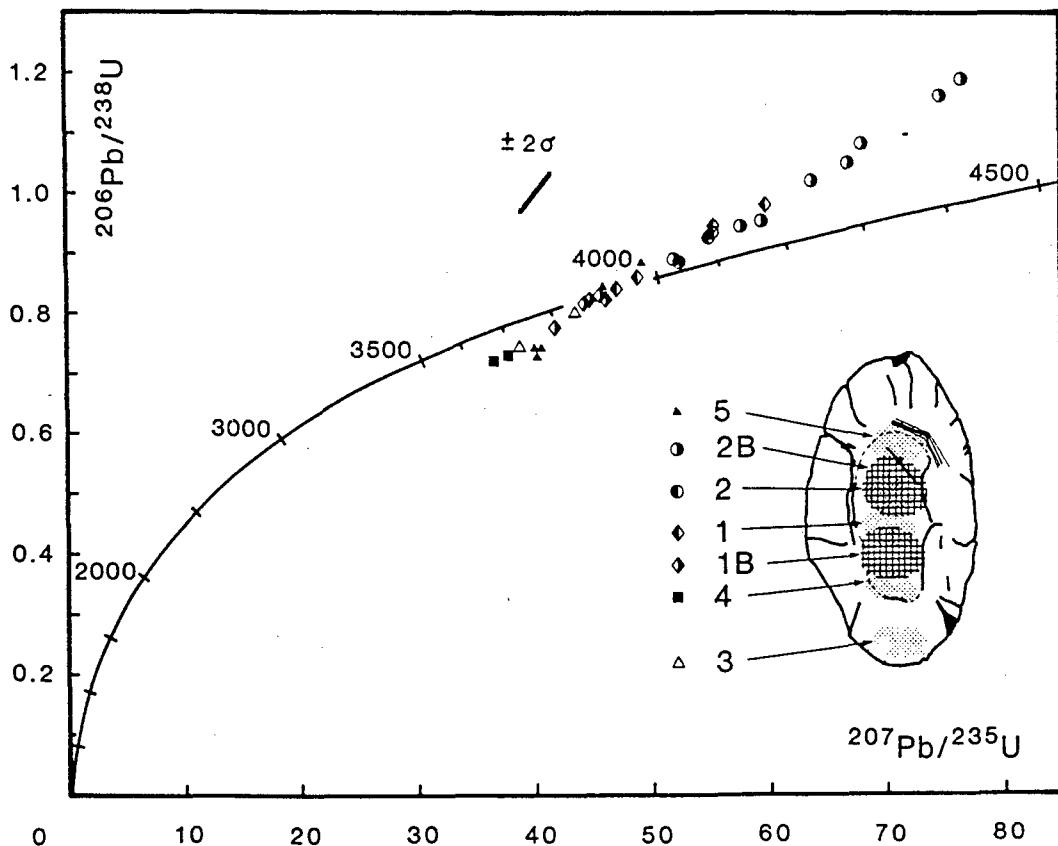
FIG. 5. Concordia plot of ion microprobe data from different regions within a single zircon grain, showing 'reverse discordance', owing to Pb gain (Williams *et al.*, 1984).

analyses, showing a concentric zoning pattern. Deloule *et al.* (1986) studied the correlation of Pb and S isotopes in galena. Meddaugh *et al.* (1982) analysed galena associated with uraninite from Elliot Lake, Ontario, Canada, containing a high proportion of radiogenic Pb. The isotope data showed the uraninite to be more than 2.1 Gyr old and indicated at least two periods of Pb loss.

Isotope anomalies in meteorites. In certain types of meteorite, anomalies occur in the isotopic abundances of various elements. These have been attributed to extinct radioactivities, mass fractionation, or imperfect mixing of primordial material from sources with varying isotope abundance patterns. The ion microprobe has played a vital part in the study of these effects, since the anomalies are localized and vary within single grains.

Excess ^{26}Mg found in anorthite in Ca–Al-rich inclusions in the Allende meteorite was first discovered, albeit in very dilute form, using con-

ventional mass spectrometry. However, the ion microprobe has enabled the true size of the anomaly to be determined as well as yielding important information on spatial distribution. Measurements by Bradley *et al.* (1978) showed ^{26}Mg abundances up to 40% above normal and a correlation with Al concentration suggesting that the excess ^{26}Mg was produced by the decay of radioactive ^{26}Al. This has important implications for early solar system chronology: ^{26}Al having a half life of only 7×10^5 years, the time interval between nucleosynthesis and the formation of the solar system may be inferred to have been not more than a few million years. These measurements were made with an ARL instrument at low mass resolution. The ^{24}Mg peak was corrected for interference from ^{48}Ca^{2+} and instrumental mass fractionation was monitored by measuring ^{25}Mg/^{24}Mg. With a Mg concentration of only around 200 ppm, the accuracy of the ^{26}Mg/^{24}Mg ratios was significantly limited by counting stat-
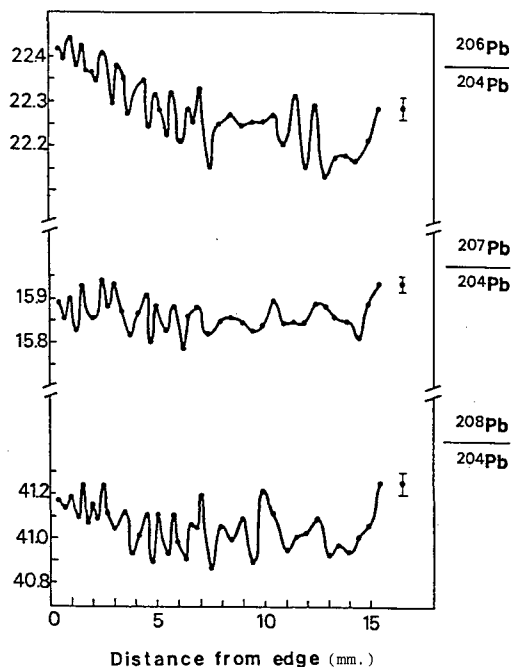
FIG. 6. Pb isotope profiles across a large galena crystal from Picher Mine (Oklahoma), showing effect of oscillatory changes in ore-forming solutions (Deloule *et al.*, 1986).

istics. Excess ^{26}Mg was also detected in Allende anorthite by Shimizu *et al.* (1978) and Okano and Nishimura (1979).

Further measurements were made by Hutcheon *et al.* (1978) and Hutcheon (1982), using an AEI instrument. Inspection of the Mg peaks at a mass resolution of 3000 confirmed the absence of interferences in anorthite other than ^{48}Ca^{2+} at mass 24, the maximum correction for which was only 3%. Measurements on terrestrial standards revealed instrumental mass fractionation of up to 0.7% per mass unit. The precision of ^{26}Mg/^{24}Mg ratios measured on Allende anorthite grains was generally better than ±0.25%. Fig. 7 shows a typical ^{26}Mg–^{27}Al 'isochron'. It was, however, found that excess ^{26}Mg was not always correlated with Al in this way. Measurements on Mg in hibonite and melilite also showed significant anomalies.

Huneke *et al.* (1983) used a Cameca IMS-3f instrument modified for high-precision isotope ratio determination. Preliminary tests showed that with carefully controlled operating conditions, enrichments in ^{26}Mg of 0.3% could be detected. Uniform mass fractionation of Mg was found in the main phases (spinel, melilite, and plagioclase)

in one Allende inclusion. Smaller but significant fractionation of Si was also observed.

Other studies of Mg isotopes in meteorites are as follows:

Macdougall and Phinney (1979)—Murchison hibonite;

Bar-Matthews *et al.* (1982)—Murchison corundum;

Clayton *et al.* (1984)—Allende forsterite;

Hinton and Bischoff (1984)—Dhajala hibonite;

Lorin and Havette (1985)—Leoville anorthite and spinel;

Ireland *et al.* (1986)—Murchison spinel;

Fahey *et al.* (1987c)—Efremovka spinel and melilite;
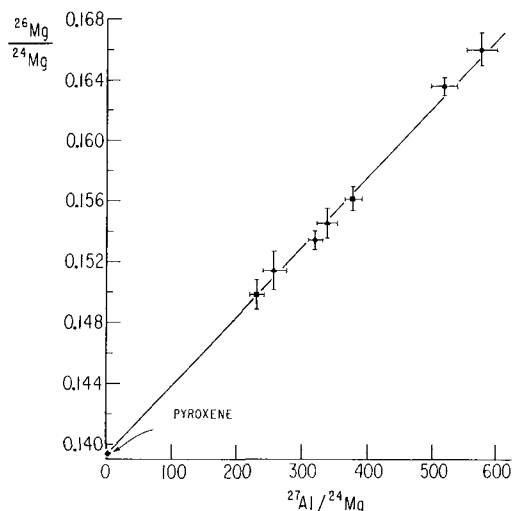
Ireland and Compston (1987)—Murchison hibonite.

FIG. 7. Mg isotope 'isochron' for anorthite in Allende meteorite, showing ^{26}Mg excess of up to 19% (correlated with Al) compared to 'normal' pyroxene (after Hutcheon, 1982).

Another element known from measurements by conventional mass spectrometry to exhibit isotope anomalies in meteorites is Ti. As in the case of Mg, much larger effects are observable with the ion probe owing to its spatial resolution. Ireland *et al.* (1985) described the application of the ANU instrument to the measurement of Ti isotope abundances in hibonite from Murchison. A mass resolution of 7000 was used, this being sufficient to separate the Ti isotopes from all molecular interferences, though not from ^{46}Ca, ^{50}V and ^{50}Cr, which were removed by a stripping procedure.

Instrumental mass fractionation, though quite large (and matrix-dependent) for Ti, was controlled to within 0.2% by using a hibonite standard mounted together with the Murchison grains. Anomalies of up to 4% were observed for ^{50}Ti, with smaller effects for the other Ti isotopes, indicating considerable heterogeneity in the source material.

Fahey et al. (1985) studied Ti isotopes in hibonite from the Murchison and Murray carbonaceous chondrites, using a Cameca IMS-3f instrument at a mass resolution of 13000 to separate ^{48}Ca from ^{48}Ti (Fig. 8). Abundances of ^{50}Ti up to 10% above normal were found. In a more extensive study, the correlation of Ti isotope anomalies with Mg isotopes, REE patterns and other trace elements was investigated (Fahey et al., 1987a). Zinner et al. (1986) found ^{48}Ca anomalies of up to about 5% associated with anomalous Ti in hibonites, suggesting incorporation of varying proportions of neutron-rich Ca and Ti carried by interstellar dust grains. Negative ^{50}Ti anomalies of several percent were observed by Hinton et al. (1987) in Murchison hibonite.
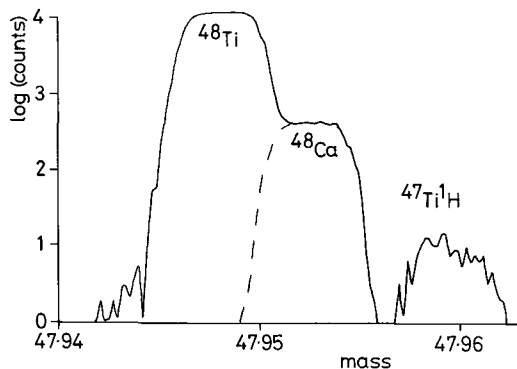

FIG. 8. Mass 48 peak from pyroxene in Allende meteorite, recorded at mass resolution of 13000 (Fahey et al., 1987a).

Armstrong and Hutcheon (1985) have described the search for ^{41}K, which is the decay product of the short-lived isotope ^{41}Ca (half-life 10^5 years). Measurements on high-Ca, low-K, fassaite enable an upper limit of 10^{-8} for the ^{41}K/^{40}Ca ratio to be determined, thereby establishing a lower limit for the time interval between nucleosynthesis and the formation of this material. The measurements are very difficult because of the low K concentration and the presence of interferences. A correction for the unresolvable ^{40}Ca^{42}Ca^{2+} inter-

ference may be derived from the intensity of the ^{40}Ca^{43}Ca^{2+} peak.

Hutcheon et al. (1987) measured isotopic abundances of Mg, Fe, Mo, Ru and W in refractory metallic inclusions ('fremdlinge') in Allende. Small mass fractionations were observed but no 'nuclear' anomalies, suggesting a solar-system origin.

The ratio of ^{7}Li to ^{6}Li is of interest as an indicator of conditions of nucleosynthesis, but in this case instrumental mass fractionation is serious, owing to the large mass difference between the isotopes. Klossa et al. (1981) measured Li isotope abundances in Allende using a Cameca IMS-300 instrument, and found no significant anomalies. An accuracy of 3% in the ^{7}Li/^{6}Li ratio was obtained (except in the case of spinel, where larger fractionation effects were encountered).

Measurements on extraterrestrial material by conventional mass spectrometry have revealed anomalies in the ratio of deuterium (^{2}H or D) to 'normal' hydrogen (^{1}H), presumably due to the presence of an exotic component. The measurement of D/H ratios with the ion probe is challenging, in view of the low abundance of D (0.015%) and the presence of large instrumental fractionation effects. However, Zinner et al. (1983) demonstrated the existence of deuterium enrichments of more than 100% in dust particles from the upper atmosphere (probably of cometary origin). A Cameca IMS-3f instrument was used, with a Cs$^+$ primary beam; negative secondary hydrogen ions were detected in order to maximize the signal. Investigation at high mass resolution showed that the ^{1}H$_2^-$ interference was negligible and the measurements were made at low mass resolution. Instrumental fractionation effects exceeding 10% were observed. McKeegan et al. (1985) found deuterium excesses of up to 250% in similar particles.

McKeegan et al. (1985) measured ^{13}C/^{12}C ratios in stratospheric dust particles, using a mass resolution of 3200 to eliminate the effect of ^{12}C^{1}H on ^{13}C. No anomalies were found. The same technique was used by Zinner and Epstein (1987) to analyse oxide particles from the Murchison meteorite, in which ^{13}C excesses of up to 700% were recorded. The ratio C_2^-/C^-, which is dependent on C concentration, was used to deduce that the C was concentrated on a micro-scale, rather than being uniformly distributed. Secondary ion images of individual grains (around 10–20 μm in size) showed C to be associated with Si, suggesting the C carrier was SiC (thought to originate from the circumstellar atmospheres of red giants). In some cases the images showed the distribution of ^{13}C to be different from ^{12}C. Similar measurements were carried out by Zinner et al. (1987) on

residues containing mostly spinel and diamond extracted from the Murray meteorite, which again showed large ^{13}C excesses. Also found were anomalies of up to 10% in Si isotopes and of up to 76% in ^{15}N. The CN$^-$ peaks were used for determining N isotopes (the N$^-$ yield being very low), with a mass resolution of 6500 in order to resolve ^{12}C^{15}N from ^{13}C^{14}N and ^{11}B^{16}O.

McKeegan (1987) carried out O isotope measurements on stratospheric dust particles, with the object of confirming their extraterrestrial origin from the presence of anomalous ^{16}O abundances, as found in certain meteorites. Cs$^+$ bombardment and negative secondary ion detection were used for maximum sensitivity; specimen charging was alleviated by mounting the particles on gold foil. A mass resolution of 8000 was used in order to separate ^{17}O from ^{16}O^{1}H. Oxygen isotope abundances were also measured by Fahey et al. (1987b) in hibonite grains from carbonaceous chondrites, which showed ^{16}O excesses of several percent. These were not correlated with anomalies in Ca and Ti isotopes, and the authors favoured refractory interstellar dust grains of varying origin as the carriers of anomalous material rather than injection from a single supernova.

Other isotopes. Relatively little work has been reported so far on radiogenic isotopes other than Pb. In the case of ^{87}Sr the ^{87}Rb interference is unresolvable and the best prospects for Sr isotope measurements are offered by low-Rb phases. Exley (1983) studied Sr isotopes in low-Rb carbonates and found the most significant molecular interferences to be Ca$_2$ and CaMgO, which were removed by stripping. Instrumental mass fractionation was around 1% per mass unit. A precision of $\pm 0.1\%$ was obtained in ^{87}Sr/^{86}Sr ratios for Sr concentrations above 5000 ppm. The ion microprobe was used by Exley and Jones (1983) for determining ^{87}Sr/^{86}Sr ratios in kimberlitic carbonates from S. Africa.

There is considerable interest in stable isotopes of elements such as C, O and S, which are fractionated in natural processes. Of these the most promising candidate for ion microprobe analysis is S, which has four isotopes, the most significant being ^{32}S (95% abundance) and ^{34}S (4% abundance). A possible molecular interference is ^{16}O$_2$ at mass 32, separation of which requires a mass resolution of 2000. Pimminger et al. (1984) showed that if an Ar$^+$ primary beam is used this interference is negligible for pure sulphides, though it may in practice occur due to the presence of small carbonate inclusions. These authors, therefore, employed a mass resolution of 5000, allowing the use of an O$_2^+$ primary beam (which was found to be more stable) and enabling the ^{33}S

peak to be measured in the presence of ^{32}S^{1}H. Instrumental mass fractionation was about 2.5% per mass unit, but with careful control of operating conditions ^{34}S/^{32}S ratios were determined to an accuracy of better than $\pm 0.3\%$. The technique was applied to the investigation of S isotope variations within single galena crystals from the Bleiberg–Kreuth district of Austria. Centre to edge variations of more than 1%, attributed to bacterial activity, were found.

Deloule et al. (1986) studied S (and Pb) isotopes in galena from Mississippi-Valley-type deposits. Bombardment by O and Ar was used and a mass resolution of 4000 employed. The S$^-$ peaks, being of sufficient intensity, were recorded in analogue mode rather than by ion counting. The reproducibility obtained was $\pm 0.1\%$ over a period of a day. Mass fractionation was around 2% per mass unit. Samples from the Picher deposit showed correlated variations in Pb and S isotopes, suggesting a common origin, with at least three separate sources. Buick Mine material also showed evidence for multiple sources of ore-forming fluids, but in this case Pb and S were not correlated.

Chaussidon et al. (1987) used O$^-$ bombardment and S$^+$ secondary ions to determine S isotope ratios in small (about 100 μm) sulphide inclusions within diamonds of presumed mantle origin. Sulphides of octahedral and platelet forms were shown to differ isotopically ($\delta^{34} = +2.3$ and $+8.2$ per mil respectively). This evidence for heterogeneity in the mantle was interpreted in terms of recycling of crustal material. Chaussidon and Demange (1988) determined S isotopes in small magmatic sulphide inclusions, monitoring the Fe, Ni and Cu peaks in order to establish the proportions of pyrrhotite, pentlandite and chalcopyrite present and hence derive the mean mass fractionation from the mass fractionation factors determined previously for the individual phases.

Eldridge et al. (1987) described the application of the SHRIMP instrument to S isotope analysis. A mass resolution of 4500 was used in order to separate ^{64}Zn^{2+} and ^{16}O$_2^+$ peaks from ^{32}S$^+$. For six different sulphide phases the ^{32}S$^+$ intensity (obtained by O$^-$ bombardment) varied by a factor of more than 4 and mass fractionation varied between 1.5% and 6% per mass unit. With a standard of the same phase as the unknown and measuring both in the same session, it was found that δ^{34} could be determined with an accuracy approaching $\pm 0.2\%$. The same procedure was used by Eldridge et al. (1988) to analyse finely intergrown sulphides from the Rammelsberg ore deposit, revealing a large isotopic difference between hydrothermal chalcopyrite and closely associated biogenic pyrite.

The determination of carbon and oxygen isotopes is more difficult owing to the greater mass fractionation and the low abundances of the minor isotopes (e.g. $^{13}C = 1.1\%$, $^{17}O = 0.04\%$, $^{18}O = 0.2\%$). In this field the application of the ion microprobe is still at an early stage of development, though considerable success has already been achieved in the analysis of 'cosmic' materials (meteorites etc.), where there are large isotopic anomalies (see previous section). The method has also been applied to diffusion measurements using isotope tracers (see below).

It is sometimes advantageous to use the ion microprobe for bulk isotopic analysis in place of a conventional mass spectrometer, especially for elements which give a low thermal ionization yield. For example, Luck et al. (1980) measured Re and Os by the isotope dilution technique in chemically separated samples from meteorites. Further results, using a refined procedure, were reported by Luck and Allègre (1983). This method has also been applied to the determination of Os isotope abundances in manganese nodules (Luck and Turekian, 1983; Palmer et al., 1988).

Depth profiling. The erosion of the sample by the bombarding ions enables the depth distribution of an element or isotope of interest to be determined by measuring the appropriate peak intensity as a function of time and converting the time scale to distance. For this purpose it is sufficient to measure the final depth of the sputtered pit (e.g. by optical interferometry), since the erosion rate can be assumed to be constant. In order to obtain a true depth profile it is necessary to produce a flat-bottomed crater and to collect secondary ions only from the central area. This can be accomplished by scanning the beam in a square raster and excluding the secondary signal from the edges ('electronic windowing'). Since the beam diameter is usually several μm, an area of several tens of μm square must be scanned and depth profiles are thus only meaningful when the sample is uniform over such an area (a condition not commonly satisfied in geological samples). The depth resolution is of the order of 10 nm. Depth profiling has been reviewed by Magee and Honig (1982) and Wittmaack (1982).

Miura and Tomisaka (1978) measured Na/Al and K/Al ratios in labradorite feldspar in the depth profiling mode, thereby establishing the range of compositions of the lamellae. An alternative approach was used by Miura and Rucklidge (1979) to analyse peristerites and crypto-perthites with lamellae too irregular for normal depth profiling; with a beam diameter of about 5 μm they analysed points along a line on the surface of a section cut at an oblique angle to the lamellae,

enabling an effective resolution of better than 1 μm to be obtained.

In a study of surface chemical changes of titanite (sphene) caused by leaching, Bancroft et al. (1987) used the specimen isolation method, as described in an earlier section, in order to suppress molecular interferences, and recorded depth profiles of a number of elements. This study was motivated by the proposed use of titanite for long-term immobilization of nuclear waste. Nesbitt and Muir (1988) used a similar approach to the investigation of the natural weathering of feldspars and observed a consistent reduction in the Si/Al ratio near the surface, probably related to the high Al content of acidic soil water.

The ion microprobe has considerable potential for the analysis of fluid inclusions, using the ion beam both to remove the solid material above the inclusion (which must be near the surface) and to analyse it. Green (1979) attempted to obtain information on the cations present in bubbles containing fluid and gaseous carbon dioxide by 'drilling' into them with the ion beam and monitoring the intensity of the relevant peaks. Positive indications of the presence of K and Ti were obtained, though these were probably on the surface of the bubbles rather than in the fluid. The prospects for obtaining meaningful analyses are greatly improved if the fluid is frozen by means of a liquid nitrogen cold stage. Nambu and Sato (1981) analysed frozen fluid inclusions in quartz and sphalerite in samples from hydrothermal ore deposits. The considerable compositional differences observed were interpreted in terms of variations in the mineralizing fluid as a function of time. Further work using this technique has been reported by Sato et al. (1984). The ability to analyse individual inclusions is a considerable advantage, especially where multiple generations are present.

Surface analysis can be regarded as a special case of depth profiling and is one of the most widely used modes of SIMS analysis outside geology. However, reported geological applications are few. Meyer et al. (1975) studied surface films on lunar particles and found enrichments in Zn, Ga, and Pb, amongst other elements, which were considered to have originated by condensation from lava fountains. In further lunar studies, Zinner et al. (1976) used a primary beam composed of NO_2^- ions at 9 keV, thereby obtaining improved depth resolution (about 3 nm) because of the relatively small kinetic energy of the individual atoms after dissociation of the NO_2^- on impact. Artificially ion-implanted standards were used, and surface concentrations of C, Mg, Cr and Fe were measured. In later work (Zinner et al., 1977, 1978) the

peaks were inspected for interferences at high mass resolution. It was concluded that observed enrichments in Fe and Mg were probably of solar wind origin, though other sources of surface enrichment appeared to be predominant for other elements.

Diffusion measurements. The ability of the ion microprobe to measure isotope ratios on small selected areas can be applied to diffusion experiments using isotope tracers. The spatial resolution of around 10 nm obtainable in the depth profiling mode (see above) helps to overcome the difficulty that the laboratory time scale is much shorter than that of natural geological processes.

In a study of K self-diffusion in biotite, Hofmann *et al.* (1974) used the ion microprobe to measure $^{39}K/^{41}K$ as a function of distance from the surface of a biotite crystal previously subjected to ion exchange with a solution enriched in ^{41}K. Depth profiles obtained at different points across the surface of the crystal indicated much faster diffusion in the direction of the *a* and *b* axes.

Ion microprobe measurements of Sr and Sm diffusion rates in diopside by Sneeringer *et al.* (1984), using the depth profiling mode were found to agree satisfactorily with results obtained by other techniques. The results were used to deduce closure temperatures for Sr and Sm movement in upper mantle material.

It is not always necessary to use depth profiling for measuring diffusion profiles; for example, Morioka (1981) determined Mg and Ca diffusivity by means of isotope tracers deposited on the surface of oriented olivine cubes and diffused at temperatures of 1000–1450 °C for 10–300 hours. The profiles extended over sufficient distance to be recorded with a 3 μm ion beam across a polished section through each cube.

Tracer diffusion coefficients for Li in albite, anorthoclase and obsidian glass were determined by Jambon and Semet (1978). Glass wafers were polished on one face, upon which a thin Li layer was deposited, diffusion anneals being carried out at 300–900 °C. After sectioning perpendicular to the original surface, profiles of ^7Li concentration were obtained. Lowry *et al.* (1981) determined tracer diffusion coefficients for Li in an alkali-basalt melt at 1300–1400 °C. The melt was contained in platinum tubes, and ^6Li was used as the tracer. The profiles extended over distances of the order of 1 cm and were measured on laterally sectioned samples. The same method was applied by Cunningham *et al.* (1983) to andesitic and pitchstone melts.

The diffusion of oxygen in silicates is of interest in relation to oxygen isotope geothermometry and solid-state creep. Ion probe measurements

of oxygen self-diffusion in several silicates were carried out by Giletti *et al.* (1978). The samples were allowed to exchange O isotopes with water enriched in ^{18}O, and the $^{18}O/^{16}O$ ratio was measured as a function of distance from the surface. Implantation of primary beam oxygen had the effect of diluting the ^{18}O in the sample with ^{16}O; this was not serious, however, because of the large ^{18}O enrichment of the introduced oxygen. The results obtained agreed well with data obtained previously by other methods.

A similar technique was used by Jaoul *et al.* (1980) to study oxygen self-diffusion in forsterite in the temperature range 1150–1600 °C. Also Farver and Giletti (1985) made measurements on amphiboles at 650–800 °C. Freer and Dennis (1982) carried out oxygen self-diffusion measurements by depth profiling. Bombardment was by Ar^+ ions and secondary O^- ions were detected. Charging of the uncoated specimens was avoided by using an electron flood gun. A typical profile is shown in Fig. 9. Measurements of oxygen self-diffusion rates in magnetite have been reported recently (Giletti and Hess, 1988).

Shimizu and Kushiro (1984) measured oxygen diffusivity in jadeite and diopside melts at high pressures (5–20 kbar), using diffusion couples of normal and ^{18}O-enriched melt. The dilution effect of the isotopically normal primary-beam oxygen
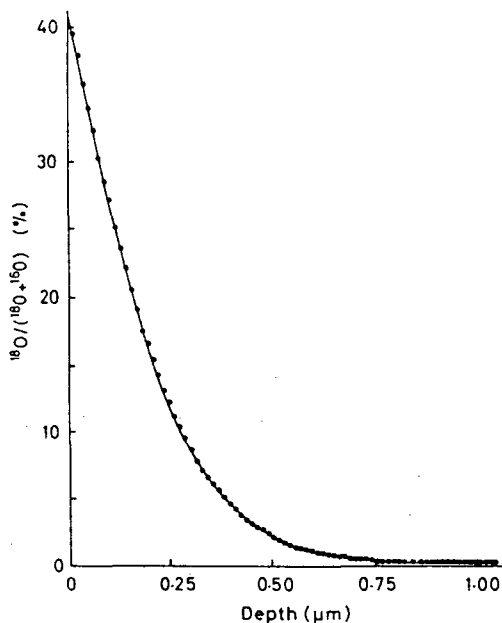

FIG. 9. Self-diffusion of O in albite: ^{18}O distribution determined by depth profiling (Freer and Dennis, 1982).

was estimated from measurements on synthetic quartz containing 50% ^{18}O. The results showed oxygen diffusivity increasing with pressure in jadeite and decreasing in diopside, demonstrating an inverse correlation with viscosity.

The ion microprobe has also been used to investigate the diffusion of water, by measuring H profiles. Delaney and Karsten (1981) determined H_2O diffusion rates in silicate glasses of various compositions, by determining the $^1H/^{16}O$ ratio as a function of distance from the edge of crystals subjected to hydration at 850 °C and 700 bars pressure for varying periods. The concentrations of H_2O at the surface were in the range 1.5–4 wt. % (well above the background level) and the profiles extended over distances of several hundred μm. Karsten et al. (1982) used the same method to determine the temperature dependence of water diffusivity in rhyolite melts.

Imaging. Secondary-ion images are principally of interest for displaying elemental distributions, the ability to image individual isotopes being useful only rarely, as in the different distributions of ^{12}C and ^{13}C in a meteorite demonstrated by Zinner and Epstein (1987). The quality of secondary-ion images is better than that of scanning X-ray images produced in the electron microprobe, owing to the higher count-rates and lower background. For major elements, reasonably noise-free images can be produced in the ion microscope type of instrument (e.g. Cameca IMS-3f/4f) with exposure times of only a few seconds. The surface sensitivity of SIMS can be a disadvantage, but may be put to good use in some applications. Interpretation of the images requires care, since matrix effects can cause differences in brightness that are unrelated to concentration.

The imaging capability of the Cameca IMS-300 was demonstrated on a sample of the Juvinas meteorite by Jérome and Slodzian (1971). Images of most of the significant elements in an area containing feldspar and two pyroxenes were recorded, with exposure times ranging from 0.5 to 10 seconds. Small Ti-rich spots were identified as rutile—a phase not previously observed in this type of meteorite.

Uranium ore samples from the Oklo natural reactor were the subject of an ion microscope study by Slodzian and Havette (1974). The UO^+ peak was used for uranium images, its intensity being much higher than that of U^+. Lead was found to be concentrated between the U-rich areas, co-existing with elements characteristic of clays. Rare earths produced by U fission were found to correlate spatially with U, indicating their immobility over long periods of time.

Lefèvre (1974) studied the distribution of a number of elements in jadeitic pyroxene of Alpine origin, while Havette and Weiss (1976) identified micro-inclusions in lava phenocrysts with the aid of ion images. Other published applications include studies of an ignimbrite from Réunion Island (Havette and Nativel, 1977) and of synthetic plagioclase feldspars by Massare et al. (1982). For a review of geological applications of imaging, see Castaing et al. (1978).

Conclusions

Ion microprobe analysis is a powerful and multifaceted technique which, in view of its unique capabilities, can be expected to play an increasingly important role in geochemical research. Its main fields of application may be summarised as follows:

(1) Light elements. The ability to detect geochemically important 'light' elements, e.g. Li, Be, B, and even H, with high sensitivity fills a significant gap left by the electron microprobe.

(2) Trace elements. Ion microprobe detection limits are generally several orders of magnitude better than are obtainable with the electron microprobe. Trace element analysis is thus possible without the need for laborious mineral separation procedures (as for neutron activation analysis, etc.), and with spatial resolution of 10 μm or better.

(3) Radiogenic isotopes. The ion microprobe can also serve as an alternative form of mass spectrometer; its advantages include rapid data acquisition with minimum sample preparation and the ability to resolve inter- and intra-grain isotopic variations. Its main application so far has been to Pb isotopes.

(4) Stable isotopes. The above-mentioned advantages are equally relevant to the study of stable isotopes of geological interest, such as S, C and O. Considerable growth can be anticipated in this field in the future.

(5) Isotope cosmochemistry. A major application is to the study of isotope anomalies in meteorites and other extraterrestrial material. Small sample consumption and high spatial resolution are important in this field.

(6) Diffusion. The ion microprobe is useful in the experimental study of diffusion in geological systems. The depth profiling mode enables very shallow profiles to be measured. Self-diffusion can be studied with isotope tracers.

(7) Depth profiling and surface analysis. The applications of these techniques include the study of weathering processes and the analysis of frozen fluid inclusions just below the surface of the sample.

(8) Imaging. The ion microprobe is superior to the electron probe for elemental imaging at low concentration levels. Also the ability to select a single isotope is occasionally useful.

Future developments. Having reviewed the present capabilities of the ion microprobe as applied to geology, it is appropriate to consider the implications of possible instrumental developments over the next few years. The routine availability of high secondary-ion transmission at high mass resolution is one very desirable goal. Though already attained in the form of the 'SHRIMP' instrument developed at the Australian National University, which incorporates a very large mass spectrometer, such an instrument is not yet available commercially. However, it may prove possible to obtain a reasonably close approximation to the performance of this instrument with a mass spectrometer of more modest size and cost, which could be made more widely available. In all cases where molecular interferences are significant, such an instrument would enable isotope ratio measurements of a given precision to be obtained in a shorter time than at present or, alternatively, a higher precision to be achieved in a comparable time. Trace element analysis times and detection limits could also be improved.

Other ways of improving sensitivity include the use of parallel detectors to record several peaks simultaneously. Another possibility is the ionization of neutral sputtered atoms after leaving the sample, or 'post-ionization' (Reuter, 1986). Using a laser tuned to an appropriate atomic resonance frequency, ion yields approaching 100% are obtainable in principle, and matrix effects are virtually eliminated. However, this promising technique has not yet been developed to the stage of routine use.

A possible alternative approach to the use of high mass resolution for dealing with molecular interferences is discrimination against molecular ions at the detector, which would enable major savings in complexity and cost to be made.

Summarizing, the ion microprobe has already demonstrated unique capabilities in a range of geological applications and has considerable further development potential. Substantial improvements in performance can be anticipated, though the cost of the equipment will continue to be a limiting factor.

References

Andersen, C. A., and Hinthorne, J. R., (1972) *Earth Planet. Sci. Lett.* **14**, 195–200.

——————(1973a) *Anal. Chem.* **45**, 1421–38.

——————(1973b) *Geochim. Cosmochim. Acta*, **37**, 745–54.

——————and Fredriksson, K. (1970) *Proc. Apollo 11 Lunar Sci. Conf.* 159–67.

Armstrong, J. T., and Hutcheon, I. D. (1985) In *Microbeam Analysis—1985* (J. T. Armstrong, ed.) San Francisco Press, 273–81.

Bancroft, G. M., Metson, J. B., Kresovic, R. A., and Nesbitt, H. W. (1987) *Geochim. Cosmochim. Acta,* **51**, 911.

Banner, A. E., and Stimpson, B. P. (1974) *Vacuum,* **24**, 511–17.

Bar-Matthews, M., Hutcheon, I. D., Macpherson, G. J., and Grossman, L. (1982) *Geochim. Cosmochim. Acta,* **46**, 31–42.

Black, L. P., Williams, I. S., and Compston, W. (1986) *Contrib. Mineral. Petrol.* **94**, 427–37.

Bradley, J. G., Huneke, J. C., and Wasserburg, G. J. (1978) *J. Geophys. Res.* **83**, 244–54.

Castaing, R., and Slodzian, G. (1962) *Microscopie,* **1**, 395–410.

——Bizouard, H., Clochiatti, R., and Havette, A. (1978) *Bull. Mineral.* **101**, 245–62.

Cerny, P., Smith, J. V., Mason, R. A., and Delaney, J. S. (1984) *Can. Mineral.* **22**, 631–51.

Chaussidon, M., and Demange, J.-C. (1988) In *Secondary Ion Mass Spectrometry—SIMS VI* (A. Benninghoven *et al.*, eds.) John Wiley, Chichester, 937–40.

——Albarède, F., and Sheppard, S. M. F. (1987) *Nature,* **330**, 242–4.

Chryssoulis, S. L., Cabri, L. J., and Salter, R. S. (1987) In *Proc. Int. Symp. on Gold Metallurgy* (R. S. Salter, D. H. Wyslouzil, and G. W. McDonald, eds.) Pergamon Press, New York, 235–44.

——Surges, L. J., and Salter, R. S. (1985) In *Complex Sulphides. Processing of Ores Concentrates and By-Products* (A. D. Zunkel, R. S. Boorman, A. E. Morris, and R. J. Wessely, eds.) AIME, Warrendale, Pa., 815–30.

——Chauvin, W. J., and Surges, L. J. (1986) *Can. Metall. Quart.* **25**, 233–59.

Claoué-Long, J. C., Compston, W., and Cowden, A. (1988) *Earth Planet. Sci. Lett.* **89**, 239–59.

Clayton, R. N., Macpherson, G. J., Hutcheon, I. D., Davis, A. M., Grossman, L., Mayeda, T. K., Molini-Velsko, C., and Allen, J. M. (1984) *Geochim. Cosmochim. Acta,* **48**, 535–48.

Compston, W., and Kröner, A. (1988) *Earth Planet. Sci. Lett.* **87**, 13–28.

——and Pidgeon, R. T. (1986) *Nature,* **321**, 766–9.

——Williams, I. S., and Clement, S. W. (1982) *Amer. Soc. for Mass Spectrom. Conf., Honolulu,* abstracts, 593–5.

——Kinny, P. D., Williams, I. S., and Foster, J. J. (1986a) *Earth Planet. Sci. Lett.* **80**, 71–81.

——Williams, I. S., Campbell, I. H., and Gresham, J. J. (1986b) Ibid. **76**, 299–311.

——————and McCulloch, M. T. (1986c) *Austral. J. Earth Sci.* **33**, 193–200.

——————Jenkins, R. F. J., Gostin, V. A., and Haines, P. W. (1987) Ibid. **34**, 435–45.

Crozaz, G., and Zinner, E. (1985) *Earth Planet. Sci. Lett.* **73**, 41–52.

Cunningham, G. J., Henderson, P., Lowry, R. K., Nolan, J., Reed, S. J. B., and Long, J. V. P. (1983) Ibid. **65**, 203–5.

Delaney, J. R., and Karsten, J. L. (1981) Ibid. **52**, 191–202.

Deloule, E., Allègre, C., and Doe, B. (1986) *Econ. Geol.* **81**, 1307–21.

Drake, M. J., Newsom, H. E., Reed, S. J. B., and Enright, M. C., (1984) *Geochim. Cosmochim. Acta,* **48**, 1609–15.

Dutrow, B. L., Holdaway, M. J., and Hinton, R. W. (1986) *Contrib. Mineral. Petrol.* **94**, 496–506.

Eldridge, C. S., Compston, W., Williams, I. S., Walshe, J. L., and Both, R. A. (1987) *Int. J. Mass Spectrom. Ion Processes,* **76**, 65–83.

—— —— Both, R. A., Walshe, J. L., and Ohmoto, H. (1988) *Econ. Geol.* **83**, 443–9.

Exley, R. A. (1983) *Earth Planet. Sci. Lett.* **65**, 303–10.

——and Jones, A. P. (1983) *Contrib. Mineral. Petrol.* **83**, 288–92.

Fahey, A., Goswami, J. N., McKeegan, K. D., and Zinner, E. (1985) *Astrophys. J.* **296**, L17–20.

—— —— —— ——(1987a) *Geochim. Cosmochim. Acta,* **51**, 329–50.

—— —— —— ——(1987b) *Astrophys. J.* **323**, L91–5.

——Zinner, E. K., Crozaz, G., and Kornacki, A. S. (1987c) *Geochim. Cosmochim. Acta,* **51**, 3215–29.

Farver, J. R., and Giletti, B. J. (1985) Ibid. **49**, 1403–11.

Freer, R., and Dennis, P. F. (1982) *Mineral. Mag.* **45**, 179–92.

Froude, D. O., Ireland, T. R., Kinny, P. D., Williams, I. S., Compston, W. Williams, I. R., and Myers, J. S. (1983) *Nature,* **304,** 616–18.

Gaudette, H. E., Vitrac-Michard, A., and Allègre, C. J. (1981) *Earth Planet. Sci. Lett.* **54**, 245–60.

Giletti, B. J., and Hess, K. C. (1988) Ibid. **89**, 115–21.

——Semet, M. P., and Yund, R. A. (1978) *Geochim. Cosmochim. Acta,* **42**, 45–57.

Green, H. W. (1979) *Nature,* **277**, 465–7.

Grew, E. S., and Hinthorne, J. R. (1983) *Science,* **221**, 547–9.

—— ——and Marquez, N. (1986) *Am. Mineral.* **71**, 1129–34.

Harrison, T. M., Aleinikoff, J. N., and Compston, W. (1987) *Geochim. Cosmochim. Acta,* **51**, 2549–58.

Hart, S. R., Shimizu, N., and Sverjensky, D. A. (1981) *Econ. Geol.* **76**, 1873–8.

Havette, A., and Nativel, P. (1977) *Bull. Soc. Fr. Mineral. Cristallogr.* **100**, 20–7.

——and Slodzian, G. (1980) *J. Physique Lett.* **41**, L247–50.

—— ——(1982) In *Secondary Ion Mass Spectrometry—SIMSIII* (A. Benninghoven et al., eds.) Springer-Verlag, Berlin, 288–91.

——and Weiss, J. (1976) *Bull. Soc. Fr. Mineral. Cristallogr.* **99**, 165–8.

Hendry, D. A. F., Chivas, A. R., Reed, S. J. B., and Long, J. V. P. (1981) *Contrib. Mineral. Petrol.* **78**, 404–12.

—— ——Long, J. V. P., and Reed, S. J. B. (1985) Ibid. **89**, 317–29.

Hervig, R. L., Kortemeier, W. T., and Burt, D. M. (1987) *Am. Mineral.* **72**, 392–6.

——Smith, J. V., Steele, I. M., and Dawson, J. B. (1980a) *Earth Planet. Sci. Lett.* **50**, 41–58.

—— —— ——Gurney, J. J., Meyer, H. O. A., and Harris, J. W. (1980b) *J. Geophys. Res.* **85B**, 6919–29.

Hinthorne, J. R., and Ribbe, P. H. (1974) *Am. Mineral.* **59**, 1123–6.

——and Andersen, C. A. (1975) Ibid. **60**, 143–7.

—— ——Conrad, R. L., and Lovering, J. F. (1979) *Chem. Geol.* **25**, 271–303.

Hinton, R. W., and Bischoff, A. (1984) *Nature,* **308,** 169–72.

——and Long, J. V. P. (1979) *Earth Planet. Sci. Lett.* **45**, 309–25.

——Davis, A. M., and Scatena-Wachel, D. E. (1987) *Astrophys. J.* **313**, 420–8.

Hofmann, A. W., Giletti, B. J., Hinthorne, J. R., Andersen, C. A., and Comaford, D. (1974) *Earth Planet. Sci. Lett.* **24**, 48–52.

Holdaway, M. J., Dutrow, B. L., Borthwick, J., Shore, P., Harmon, R. S., and Hinton, R. W. (1986) *Am. Mineral.* **71**, 1135–41.

Huneke, J. C., Armstrong, J. T., and Wasserburg, G. J. (1983) *Geochim. Cosmochim. Acta,* **47**, 1635–50.

Hutcheon, I. (1982) In *Nuclear and Chemical Dating Techniques: Interpreting the Environmental Record* (L. A. Curie, ed.), Am. Chem. Soc. Symp. Series no. 176, 95–128.

——Armstrong, J. T., and Wasserburg, G. J. (1987) *Geochim. Cosmochim. Acta,* **51**, 3175–92.

——Steele, I. M., Smith, J. V., and Clayton, R. N. (1978) *Proc. 9th Lunar Planet. Sci. Conf.,* 1345–68.

Ireland, T. R., and Compston, W. (1987) *Nature,* **327**, 689–92.

—— ——and Heydegger, H. R. (1985) *Geochim. Cosmochim. Acta,* **49**, 1989–93.

—— ——and Esat, T. M. (1986) Ibid. **50**, 1413–21.

Jambon, A., and Semet, M. P. (1978) *Earth Planet. Sci. Lett.* **37**, 445–50.

Jaoul, O., Froidevaux, C., Durham, W. B., and Michaut, M. (1980) Ibid. **47**, 391–7.

Jérome, D. Y., and Slodzian, G. (1971) *Bull. Soc. Fr. Mineral. Crystallogr.* **94**, 538–48.

Jones, A. P., and Smith, J. V. (1984) *Neues Jahrb. Mineral. Mh.* 228–40.

Karsten, J. L., Holloway, J. R., and Delaney, J. R. (1982) *Earth Planet. Sci. Lett.* **59**, 420–8.

Kinny, P. D. (1986) Ibid. **79**, 337–47.

——Williams, I. S., Froude, D. O., Ireland, T. R., and Compston, W. (1988) *Precamb. Res.* **38**, 325–41.

Klossa, B., Pierre, A., and Minster, J.-F. (1981) Ibid. **52**, 25–30.

Kröner, A., and Compston, W. (1988) Ibid. **38**, 367–80.

—— ——Guo-wei, Z., An-lin, G., and Todt, W. (1988a) *Geology,* **16**, 211–15.

——Wendt, I., Liew, T. C., Compston, W., Todt, W., Fiala, J., Vankova, V., and Vanek, J. (1988b) *Contrib. Mineral. Petrol.* **99**, 257–66.

Lefèvre, R. (1974) *Bull. Soc. Geol. Fr.* **16**, 248–54.

Lepareur, M. (1980) *Rev. Technol. Thomson-CSF* **12**, 225–65.

Leta, D. P., and Morrison, G. H. (1980) *Anal. Chem.* **52,** 277–80.

Liebl, H. (1967) *J. Appl. Phys.* **38,** 5277–83.

Lorin, J. C., and Havette, A. (1985) In *Rapports Isotopique dans le Systeme Solaire,* Cepadue-Editions, Paris, 1–27.

——— and Slodzian, G. (1982) In *Secondary Ion Mass Spectrometry—SIMSIII* (A. Benninghoven *et al.,* eds.) Springer-Verlag, Berlin, 140–50.

Lovering, J. F. (1975) In *Secondary Ion Mass Spectrometry* (K. F. J. Heinrich and D. E. Newbury, eds.) Nat. Bur. Stands. spec. publ. 427, U.S. Dept. of Commerce, Washington, 135–78.

———Travis, G. A., Comaford, D. J., and Kelly, P. R. (1981) In *Archaean Geology—2nd International Symposium, Perth, 1980* (J. E. Glaser and D. I. Groves, eds.) Spec. Publ. Geol. Soc. Austral. **7,** 193–203.

Lowry, R. K., Reed, S. J. B., Nolan, J., Henderson, P., and Long, J. V. P. (1981) *Earth Planet Sci. Lett.* **53,** 36–40.

Luck, J.-M., and Allègre, C. J. (1983) *Nature,* **302,** 130–2.

——— and Turekian, K. K. (1983) *Science,* **222,** 613–15.

———Birck, J.-L., and Allègre, C. J. (1980) *Nature,* **283,** 256–9.

Macdougall, J. D., and Phinney, D. (1979) *Geophys. Res. Lett.* **6,** 215–18.

McIntyre, N. S., Cabri, L. J., Chauvin, W. J., and Laflamme, J. H. G. (1984) *Scanning Elect. Microsc./1984,* 1139–46.

McKeegan, K. D. (1987) *Science,* **237,** 1468–71.

———Walker, R. M., and Zinner, E. (1985) *Geochim. Cosmochim. Acta,* **49,** 1971–87.

MacRae, N. D. (1987) *Am. Mineral.* **72,** 1263–8.

———Metson, J. B. (1985) *Chem. Geol.* **53,** 325–33.

———Russell, M. R. (1987) Ibid. **64,** 307–17.

Magee, C. W., and Honig, R. E. (1982) *Surf. Interface Anal.* **4,** 35–41.

Mason, R. A. (1982) *Mineral. Mag.* **45,** 101–6.

———(1987) *Chem. Geol.* **64,** 209–24.

———Smith, J. V., Dawson, J. B., and Treves, S. B. (1982) Ibid. **46,** 7–11.

———Parsons, I., and Long, J. V. P. (1985) *J. Petrol.* **26,** 952–70.

Massare, D., Havette, A., and Slodzian, G. (1982) *J. Microsc. Spectrosc. Electron,* **7,** 477–86.

Meddaugh, W. S., Holland, H. D., and Shimizu, N. (1982) In *Ore Genesis* (G. C. Amstutz *et al.,* eds.) Springer-Verlag, Berlin, 25–37.

Meyer, C. (1978) *Proc. 9th Lunar Planet. Sci. Conf.* 1551–70.

———Anderson, D. H., and Bradley, J. G. (1974) *Proc. 5th Lunar Sci. Conf.* 685–706.

———McKay, D. S., Anderson, D. H., and Butler, P. (1975) *Proc. 6th Lunar Sci. Conf.* 1673–99.

Migeon, H. N., Le Pipec, C., and Le Goux, J. J. (1986) In *Secondary Ion Mass Spectrometry—SIMS V* (A. Benninghoven *et al.,* eds.) Springer-Verlag, Berlin, 155–7.

Mitchell, R. H., and Reed, S. J. B. (1988) *Mineral. Mag.* **52,** 331–9.

Miura, Y., and Rucklidge, J. C. (1979) *Am. Mineral.* **64,** 1272–9.

———and Tomisaka, T. (1978) Ibid. **63,** 584–90.

Morioka, M. (1981) *Geochim. Cosmochim. Acta,* **45,** 1573–80.

Muir, I. J., Bancroft, G. M., MacRae, N. D., and Metson, J. B. (1987) *Chem. Geol.* **64,** 269–78.

Nambu, H., and Sato, T. (1981) *Bull. Mineral.* **104,** 827–33.

Nesbitt, H. W., and Muir, I. J. (1988) *Nature,* **334,** 336–8.

———Metson, J. B., and Bancroft, G. M. (1986) *Chem. Geol.* **55,** 139–60.

Okano, J., and Nishimura, H. (1979) In *Secondary Ion Mass Spectrometry—SIMSII* (A. Benninghoven *et al.,* eds.) Springer-Verlag, Berlin, 216–18.

———(1982) In *Secondary Ion Mass Spectrometry—SIMSIII* (A. Benninghoven *et al.,* eds.) Springer-Verlag, Berlin, 426–30.

———and Uyeda (1988) In *Secondary Ion Mass Spectrometry—SIMS VI* (A. Benninghoven *et al.,* eds.) John Wiley, Chichester, 941–4.

Palmer, M. R., Falkner, K. K., Turekian, K. K., and Calvert, S. E. (1988) *Geochim. Cosmochim. Acta,* **52,** 1197–202.

Phinney, D., Whitehead, B., and Anderson, D. (1979) Proc. 10th Lunar Sci. Conf. 885–905.

Pimminger, M., Grasserbauer, M., Schroll, E., and Cerny, I. (1984) *Anal. Chem.* **56,** 407–11.

Ray, G., and Hart, S. R. (1982) *Int. J. Mass Spectrom. Ion Phys.* **44,** 231–55.

———Shimizu, N., and Hart, S. R. (1983) *Geochim. Cosmochim. Acta,* **47,** 2131–40.

Reed, S. J. B. (1981) In *Microbeam Analysis—1981* (R. H. Geiss, ed.) San Francisco Press, 87–90.

———(1983) *Int. J. Mass Spectrom. Ion Processes,* **54,** 31–40.

———(1985) *Chem. Geol.* **48,** 137–43.

———(1986) *Mineral. Mag.* **50,** 3–15.

———and Enright, M. C. (1981) *Proc. Royal Soc. Lond.* A374, 195–205.

———and Smith, D. G. W. (1985) *Earth Planet. Sci. Lett.* **72,** 238–44.

———Scott, E. R. D., and Long, J. V. P. (1979) Ibid. **43,** 5–12.

———Smith, D. G. W., and Long, J. V. P. (1983) *Nature,* **306,** 172–3.

———Trueman, N. A., and Long, J. V. P. (1988) In *Secondary Ion Mass Spectrometry—SIMSVI* (A. Benninghoven *et al.,* eds.) John Wiley, Chichester, 945–8.

Reuter, W. (1986) In *Secondary Ion Mass Spectrometry—SIMSV* (A. Benninghoven *et al.,* eds.) Springer-Verlag, Berlin, 94–102.

Rudnick, R. L., and Williams, I. S. (1987) *Earth Planet. Sci. Lett.* **85,** 145–61.

Sato, T., Nambu, M., and Omori, Y. (1984) In *Secondary Ion Mass Spectrometry—SIMSIV* (A. Benninghoven *et al.,* eds.) Springer-Verlag, Berlin, 471–4.

Shimizu, N. (1978) *Earth Planet. Sci. Lett.* **39,** 398–406.

———(1981) *Nature,* **289,** 575–7.

———and Allègre, C. J. (1978) *Contrib. Mineral. Petrol.* **67,** 41–50.

———and Hart, S. R. (1982) *J. Appl. Phys.* **53,** 1303–11.

Shimizu, N. and Kushiro, I. (1984) *Geochim. Cosmochim. Acta*, **48**, 1295–303.

—— and Le Roex, A. P. (1986) *J. Volcan. Geotherm. Res.* **29**, 159–88.

—— and Richardson, S. H. (1987) *Geochim. Cosmochim. Acta*, **51**, 755–8.

—— Semet, M. P., and Allègre, C. J. (1978) Ibid. **42**, 1321–34.

Slodzian, G. (1982) In *Secondary Ion Mass Spectrometry—SIMSIII* (A. Benninghoven *et al.*, eds.) Springer-Verlag, Berlin, 115–23.

—— and Havette, A. (1974) *Adv. Mass Spectrom.* **6**, 629–36.

—— Lorin, J. C., and Havette, A. (1980) *J. Physique Lett.* **41**, L555–8.

Sneeringer, M., Hart, S. R., and Shimizu, N. (1984) *Geochim. Cosmochim. Acta*, **48**, 1589–608.

Steele, I. M., and Lindstrom, D. J. (1981) Ibid. **45**, 2177–83.

—— Hutcheon, I. D., and Smith, J. V. (1980a) *Proc. 11th Lunar Sci. Conf.* 571–90.

—— —— (1980b) In *X-ray Optics and Microanalysis* (D. R. Beaman *et al.*, eds.) Pendell Publ. Co., Midland, Mich., 515–25.

—— Hervig, R. L., Hutcheon, I. D., and Smith, J. V. (1981) *Am. Mineral.* **66**, 526–46.

Streit, L. A., Hervig, R. L., and Williams, P. (1986) In *Microbeam Analysis—1986* (A. D. Romig and W. F. Chambers, eds.) San Francisco Press, 91–4.

Tamura, H., Kondo, T., Doi, H., Omura, I., and Taya, S. (1970) In *Recent Developments in Mass Spectrometry* (K. Ogata and T. Hayakawa, eds.) Univ. Tokyo Press, 205–9.

Vander Wood, T. B., and Clayton, R. N. (1985) *J. Geol.* **93**, 251–70.

Veizer, J., Hinton, R. W., Clayton, R. N., and Lerman, A. (1987) *Chem. Geol.* **64**, 225–37.

Williams, I. S., and Claesson, S., (1987) *Contrib. Mineral. Petrol.* **97**, 205–17.

—— Compston, W., Black, L. P., Ireland, T. R., and Foster, J. J. (1984) Ibid. **88**, 322–7.

Wilson, G. C., and Long, J. V. P. (1982) *Int. J. Mass Spectrom. Ion Phys.* **42**, 63–75.

—— —— (1983) *Mineral. Mag.* **47**, 191–9.

Wittmaack, K. (1982) *Radiation Eff.* **63**, 205–18.

Zinner, E., and Crozaz, G. (1986) *Int. J. Mass Spectrom. Ion Processes*, **69**, 17–38.

—— and Epstein, S. (1987) *Earth Planet. Sci. Lett.* **84**, 359–68.

—— and Walker, R. M. (1975) *Proc. 6th Lunar Sci. Conf.* 3601–17.

—— Walker, R. M., Chaumont, J., and Dran, J. C. (1976) *Proc. 7th Lunar Sci. Conf.* 953–84.

—— —— —— (1977) *Proc. 8th Lunar Sci. Conf.* 3859–83.

—— Dust, S., Chaumont, J., and Dran, J. C. (1978) *Proc. 9th Lunar Sci. Conf.* 1667–86.

—— McKeegan, K. D., and Walker, R. M. (1983) *Nature*, **305**, 119–21.

—— Fahey, A. J., Goswami, J. N., Ireland, T. R., and McKeegan, K. D. (1986) *Astrophys. J.* **311**, L103–7.

—— Ming, T., and Anders, E. (1987) *Nature*, **330**, 730–2.